

# Topological signatures of periodic-like signals

FRÉDÉRIC CHAZAL<sup>1,a</sup>, BERTRAND MICHEL<sup>2,c</sup> and WOJCIECH REISE<sup>1,b</sup>

<sup>1</sup>*DataShape, Inria Saclay, Institut Mathématique d’Orsay, 307 Rue Michel Magat, 91400 Orsay, France,*

<sup>a</sup>*frederic.chazal@inria.fr,* <sup>b</sup>*reisewojciech@gmail.com*

<sup>2</sup>*Nantes Université, Centrale Nantes, Laboratoire de Mathématiques Jean Leray, CNRS UMR 6629, 1 Rue de La Noë, 44321 Nantes, France,* <sup>c</sup>*bertrand.michel@ec-nantes.fr*

We present a method to construct signatures of periodic-like data. Based on topological considerations, our construction encodes information about the order and values of local extrema. Its main strength is robustness to reparametrization of the observed signal, so that it depends only on the form of the periodic function. The signature converges as the observation contains increasingly many periods. We show that it can be estimated from the observation of a single time series using bootstrap techniques.

**Keywords:** Dependent data; functional data; limit theorems; persistent homology; time series

## 1. Introduction

We consider the problem of constructing a descriptor of a periodic function  $\phi : \mathbb{R} \rightarrow \mathbb{R}$ , based on an observation of a reparameterized and noisy signal. Specifically, we assume that  $\phi$  is 1-periodic and we let  $\gamma : [0, T] \rightarrow [0, R]$  be an increasing bijection. We consider an observation  $S$  of the form

$$S : [0, T] \rightarrow \mathbb{R}, \quad t \mapsto (\phi \circ \gamma)(t) + W(t), \quad (1)$$

where  $W = (W_t)_{t \in [0, T]} = (W(t))_{t \in [0, T]}$  is a stochastic noise process. Our aim is to construct a signature  $F : S \mapsto F(S)$  which contains information about  $\phi$  while remaining robust to  $W$  and to changes in  $\gamma$ . Such information concerns the form of the period: for instance, it could be the number of local extrema or their values. In a noiseless scenario, these are characteristic of the period of  $\phi$  and, to a certain extent, do not change with  $\gamma$ . To illustrate this objective more concretely, let us consider the two signals  $\phi_0$  and  $\phi_1$  on the top of Figure 1 and the two parametrization functions  $\gamma_0$  and  $\gamma_1$  on the left of Figure 1. We would like to define a signature  $F$  such that  $F(\phi_0 \circ \gamma_0 + W)$  is more similar to  $F(\phi_0 \circ \gamma_1 + W)$  than to  $F(\phi_1 \circ \gamma_0 + W)$ , because the former are both observations of  $\phi_0$ , and despite the fact that  $\phi_0 \circ \gamma_0$  and  $\phi_0 \circ \gamma_1$  feature three and four periods of  $\phi_0$  respectively.

Time series or functional observations of the form (1) appear in many applications, where  $\phi$  is somehow characteristic of a population: child growth dynamics (Ramsay and Silverman, 2002), physiological signals (Goldberger et al., 2000), bird migration curves (Su et al., 2014). The reparametrization  $\gamma$  is the main source of variability in the point-wise evaluations of the signals, as in the ‘phase variation’ model in Functional data analysis (FDA), see Marron et al. (2015) for a review. The problems typically considered in FDA consist in aligning a population of curves or computing a representative curve, for which methods with guarantees have been proposed (Khorram, McInnis and Provost, 2019, Tang and Müller, 2008, Wang and Gasser, 1997). Underlying most of the models is the assumption that the start and end points ( $\gamma(0)$  and  $\gamma(T)$  here) are common for all curves.

In applications like magnetic odometry or gait analysis studied in Bonis et al. (2024), Reise (2023) and Bois et al. (2022) respectively, a single observation is composed of several periods of  $\phi$  and the number of periods varies across observations. In Reise (2023), the signal  $S$  is the magnetic signal recorded in a moving car and the problem consists in inferring its displacement. The periodic function

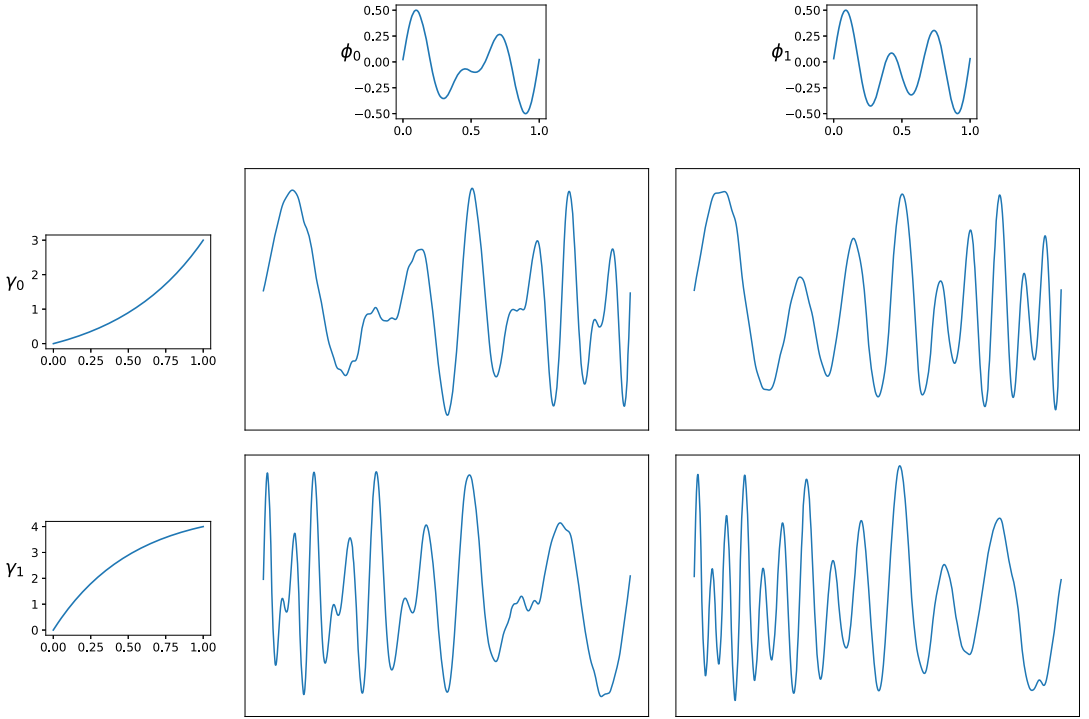


**Figure 1.** Four signals  $S_{i,j} = \phi_j \circ \gamma_i + W$  for  $i, j \in \{0, 1\}$ , for periodic functions  $\phi_0, \phi_1$  and reparametrizations  $\gamma_0, \gamma_1$ , corrupted by additive noise.

$\phi$  models the magnetic signature of the angular position,  $\gamma$ , of a wheel of that car. The problem consists in estimating  $\gamma$  from  $S$ . There is little reason for two observations to have the same number of periods, unless the initial angular position of the wheel and the trajectory are exactly the same across those two observations. Therefore, in contrast with FDA, the assumption of common endpoints is not satisfied and the problem changes from describing the whole signal, to that of describing its constituent parts, that is, the periods of  $\phi$ .

Techniques from topological data analysis (TDA) are said to describe the ‘shape of data’ and have been increasingly used to extract geometric or topological information from observations (Chazal and Michel, 2021). The arguably most popular TDA technique for analyzing a time series consists in computing the homology of the time-delay embedding (TDE) of the time series, in order to verify whether the underlying phenomenon is periodic or not (Perea, 2019). In applications, it has also been used to understand dynamical systems behind climate change (Ghil and Sciamarella, 2023), to identify market crashes (Gidea and Katz, 2018) or to propose biomarkers to detect seizures (Fernández and Mateos, 2022). The TDE of a time series  $\mathbf{X} = (X_n)_{n=1}^N$  is a point cloud in  $\mathbb{R}^d$ , where each point is of the form  $(X_n, X_{n+\tau}, \dots, X_{n+(d-1)\tau})$  for parameters  $d, \tau \in \mathbb{N}$ . If  $S$  is periodic, a simplicial complex constructed on the TDE at the right scale will have a non-trivial homology group in dimension one. In signals with phase variation however, the length of the periodic structure changes and so does the geometry of the TDE. This is corroborated by the fact that the geometry of the delay embedding contains information about the frequencies supporting the signal (Perea, 2019, section 5).

Techniques other than the TDE have been proposed to extract topological information from time series. In Corcoran and Jones (2017), the swarm behavior over time has been described with the zig-

zag persistent homology of sublevel sets of a density estimator. In [Khasawneh and Munch \(2016\)](#), the authors count revolutions of a machine in an industrial process by counting the number of ‘significant’ changes in a binary signal, where the significance of a change is defined in terms of persistence of homology generators.

Visual features like local extrema or inflection points ([Perng et al., 2000](#)) quantify the ‘shape of a curve’. Local extrema and excursion sets are particularly useful, since they are invariant to the reparametrization of the domain. We propose to use the persistent homology of sublevel sets of the signal to describe this last. This descriptor, the persistence diagram, summarizes the height, order and number of local extrema.

In many statistical applications, it is convenient to map a persistence diagram to a vector or a function, via a functional representation. Numerous functionals ([Adams et al., 2017](#), [Carrière et al., 2020](#)) are ‘linear in the diagram’ and their properties have been well-studied in [Divol and Polonik \(2019\)](#). In our case, it seems natural to renormalize the functionals by the total persistence of the diagram, a proxy for the unknown number of periods. Building on [Divol and Polonik \(2019\)](#) and a recent characterization of the stability of total persistence for Hölder regular processes from [Perez \(2022\)](#), we study the robustness of the signatures we propose.

Guarantees on the estimation of functionals of persistence diagrams, in both asymptotic and non-asymptotic cases, have been provided in [Berry et al. \(2020\)](#), [Chazal et al. \(2014\)](#), under the assumption that the persistence diagrams (or functionals thereof) in the collection are all independent. In a setting motivated by magnetic odometry problem ([Bonis et al., 2024](#)), we have a single time series of which we would like to estimate the signature. The natural procedure is to construct a sample by taking contiguous vectors from that observation, what leads to a collection of shorter and dependent observations. We study two reparametrization models and, building on the theory of strong mixing ([Dedecker et al., 2007](#), [Doukhan, 1994](#)), we show that the dependence between observations decreases. When the  $\beta$ -mixing coefficients decrease sufficiently fast, the estimators of the functionals also converge in the dependent setting ([Bühlmann, 1995](#), [Kosorok, 2008](#), [Radulović, 1996](#)), not unlike in the independent case ([Chazal et al., 2014](#)). So far, estimation of topological signatures from dependent data has been less explored: a concentration inequality for persistent Betti numbers from dependent data is derived in [Krebs \(2021\)](#).

## Contributions and outline

In this article, we propose a signature of data of the form (1). The signature captures information about local extrema and excursion sets. It is defined in the language of persistent homology of sublevel sets of a one-dimensional function. Our contribution is an analysis which covers the entire process, from data generation to a bootstrap procedure.

1. By analysing the noiseless case  $W = 0$ , we show that the proposed signature is a relevant descriptor. First, the topological functional used in the signature converges as the number of periods in a signal increases (Theorem 2.14). Second, by construction, it is invariant to reparametrization.
2. We discuss the invariance of the signature to parametrization  $\gamma$  in presence of noise. When the endpoints  $\gamma(0)$  and  $\gamma(T)$  of the parametrization  $\gamma$  are fixed, an assumption common in FDA, we show that the signature is continuous with respect to the distribution of  $\gamma$  (Theorem 3.5).
3. We consider the problem of estimating the signature from stationary time-series data. When the reparametrization satisfies Markovian properties, we exploit the periodicity of  $\phi$  to generate a sample to estimate the signature.

In Section 4, we provide a simple numerical illustration of the signature and its invariance properties.

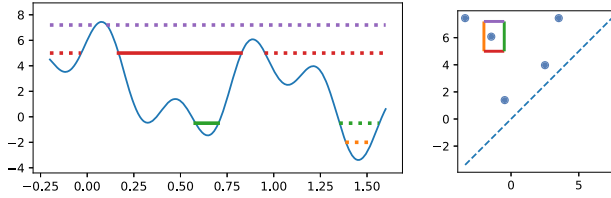


**Figure 2.** On the left, the graph of a function  $h$  and four sublevel sets marked with colors. At each level, there is a different number of connected components. The right panel shows the persistence diagram  $D(h)$ . The point contained in the interior of the small rectangle corresponds to the connected component marked in a solid line on the left panel.

## 2. Persistence diagrams of sublevel sets and functionals thereof

The signatures we propose are based on excursions sets of stochastic processes. The construction uses the theory of persistent homology, which we describe in the deterministic setting in this section. We first introduce a truncated version of persistence to keep boundedness and guarantee continuity of the persistence-based signatures introduced further. Motivated by some additivity property of persistence when studying periodic signals, we consider signatures which are normalized by the total persistence. The objects studied in this section are interesting in themselves. We will therefore adopt a more general setting than the specific model (1).

### 2.1. Persistence diagrams and total truncated persistence

In this section, we briefly recall the basics of ordinary persistence theory. A more formal presentation of persistent diagrams based on terminated persistence modules is given in the proof of Lemma 2.5.

Let  $h \in C(\mathbb{X}, \mathbb{R})$  be a continuous function on a compact topological space  $\mathbb{X}$ . The  $\alpha$ -sublevel set of  $h$  on  $\mathbb{X}$  is then defined as:  $\mathbb{X}_\alpha = \{x \in \mathbb{X} : h(x) \leq \alpha\}$ . Generally speaking, ordinary persistence keeps track of the times of appearance and disappearance of topological features in the sequence of spaces  $(\mathbb{X}_\alpha)_{\alpha \in \mathbb{R}}$ . In general, these features can be connected components, loops, cavities, etc. In this work,  $\mathbb{X} \subset \mathbb{R}$  so we focus on connected components (0-dimensional features). To fix the ideas, assume that we store the value  $\alpha_b$ , called the *birth time*, for which a new connected component appears in  $\mathbb{X}_{\alpha_b}$ . This connected component eventually gets merged with another one for some value  $\alpha_d \geq \alpha_b$ , which is stored as well and called the *death time*. Moreover, one says that the component *persistent* on the corresponding interval  $[\alpha_b, \alpha_d]$ . This family of intervals is called the barcode, or *persistence diagram*, of  $(\mathbb{X}, h)$ , and can be represented as a multiset of points (i.e., point cloud where points are counted with multiplicity) supported on  $\mathbb{R}^2$  with coordinates  $\{(\alpha_b, \alpha_d)\}$ . Throughout this work, the persistence diagram of  $h$  will be denoted by  $D(h)$  or  $D_h$ , as  $\mathbb{X}$  is always the domain of  $h$ . See Figure 2 for an illustration.

Since the persistence diagram captures information about the number of connected components and how they evolve, it does not depend on the parametrization of the domain.

**Lemma 2.1 (Invariance to reparametrization).** *Consider a continuous function  $f : \mathbb{R} \rightarrow \mathbb{R}$  and let  $\gamma_1, \gamma_2 : [0, T] \rightarrow \mathbb{R}$  be two increasing and continuous functions, such that  $\gamma_1(0) = \gamma_2(0)$  and  $\gamma_1(T) = \gamma_2(T)$ . Then,*

$$D(f \circ \gamma_1) = D(f \circ \gamma_2).$$

Lemma 2.1 is a consequence of the fact that  $\gamma_2 \circ \gamma_1^{-1}$  bijectively maps the connected components of  $f \circ \gamma_1$  to those of  $f \circ \gamma_2$ .

**Proof.** For any  $t \in \mathbb{R}$ , the homeomorphism  $g := (\gamma_1^{-1} \circ \gamma_2) : [0, T] \rightarrow [0, T]$  maps the  $t$ -sublevel set of  $f \circ \gamma_2$  to  $f \circ \gamma_1$ . Indeed,

$$\begin{aligned} (f \circ \gamma_1)^{-1}((-\infty, t]) &= \{y \in [0, T] \mid (f \circ \gamma_1)(y) \leq t\} \\ &= \{y = g(x) \mid (f \circ \gamma_1)(g(x)) = (f \circ \gamma_2)(y) \leq t\} \\ &= g(\{y \in [0, T] \mid (f \circ \gamma_2)(y) \leq t\}). \end{aligned}$$

Therefore,  $g$  induces an isomorphism between the two corresponding persistence modules. So the corresponding persistence diagrams are the same (as well as any invariants there-of).  $\square$

Persistence diagrams are also stable with respect to the filter function. One distance which is often used to compare diagrams is the bottleneck distance

$$d_b(D_1, D_2) = \inf_{\Gamma} \sup_{x \in D_1 \cup \Delta} \|x - \Gamma(x)\|_{\infty},$$

where  $\Gamma : D_1 \cup \Delta \rightarrow D_2 \cup \Delta$  is a partial bijection between the two diagrams, which allows some points to be matched to the diagonal  $\Delta$ . With respect to the supremum norm between functions, the persistence diagram is stable in that distance.

**Theorem 2.2 (Chazal et al. (2016), Cohen-Steiner, Edelsbrunner and Harer (2007)).** For two functions  $f, g : \mathbb{X} \rightarrow \mathbb{R}$  with persistence diagrams  $D_f$  and  $D_g$  respectively,

$$d_b(D_f, D_g) \leq \|f - g\|_{\infty}.$$

The persistence of  $(b, d) \in \mathbb{R}^2$  is  $w(b, d) := d - b$ . For  $p \in \mathbb{N}^+$ , the total  $p$ -persistence of a persistence diagram  $D$  is the sum of  $p$ -powers of the lifetimes of points,

$$\text{pers}_p(D) = \left( \sum_{(b, d) \in D} w(b, d)^p \right)^{1/p}.$$

It is similar to total variation for functions on the interval (Plonka and Zheng, 2016). Similarly to total variation, the total  $p$ -persistence of an  $\alpha$ -Hölder functions is finite for  $p > 1/\alpha$ , but it is not continuous for functions with regularity strictly less than Lipschitz (Perez, 2022). To keep boundedness and guarantee continuity, we introduce the *truncated persistence*,  $w_{\epsilon}(b, d) := (d - b - \epsilon)_+$ , where  $(a)_+ = \max(a, 0)$  denotes the positive part and  $\epsilon > 0$  is fixed. For  $\epsilon > 0$ , the  $\epsilon$ -truncated total  $p$ -persistence is

$$\text{pers}_{p, \epsilon}(D) = \left( \sum_{(b, d) \in D} w_{\epsilon}(b, d)^p \right)^{1/p},$$

and  $\text{supp}(w_{\epsilon}) \subset \Delta_{\epsilon} := \{(b, d) \in \mathbb{R}^2 \mid d - b \geq \epsilon\}$ .

We first give two general results on the truncated persistence of continuous functions defined on an interval, before focusing to the case of periodic functions. In the statement of Proposition 2.3, both  $f$  and  $g$  are deterministic functions.

**Proposition 2.3 (Lower- and upper-bound on  $\epsilon$ -truncated  $p$ -persistence).** *For continuous functions  $f, g : [0, T] \rightarrow \mathbb{R}$ , and for  $p > 0$ ,  $\epsilon > 0$ ,*

$$\text{pers}_{p,\epsilon}^p(f + g) \geq \text{pers}_{p,\epsilon+A_g}^p(f),$$

where  $A_g = \max g - \min g$ . In addition, if  $f$  is  $\alpha$ -Hölder function with constant  $\Lambda$  and the exponent satisfies  $(p-1)\alpha > 1$ , then

$$\text{pers}_{p,\epsilon}^p(f) \leq (A_f - \epsilon)_+^p \left( 1 + pT \left( \frac{2\Lambda}{\epsilon} \right)^{1/\alpha} \right) =: C_{p,\Lambda,\alpha,T}.$$

The result is weak but it is tight. For example, for the lower-bound, if we take  $f$  such that  $\max f - \min f = 2\|f\|_\infty$  and  $g = -\alpha f$ , then  $f + g = (1 - \alpha)f$  and  $\|g\|_\infty = \alpha\|f\|_\infty$ , so that  $\text{pers}_{p,\epsilon}^p((1 - \alpha)f) = \text{pers}_{p,\epsilon+2\alpha}^p(f)$ .

**Proof.** We start with the lower-bound. Since  $\text{pers}$  is translation-invariant ( $\text{pers}_{p,\epsilon}(f + c) = \text{pers}_{p,\epsilon}(f)$ , for any constant  $c > 0$ ), we can assume that  $A_g = 2\|g\|_\infty$ . Let  $\Gamma : D(f) \rightarrow D(f + g)$  be a matching between the diagrams and denote by  $c(\Gamma)$  the associated cost. Thanks to the bottleneck stability theorem,  $\inf_\Gamma c(\Gamma) \leq \|g\|_\infty$ . Then, for any  $(b, d) \in D(f)$  and  $(b', d') = \Gamma((b, d)) \in D(f + g)$ , we have  $d' - b' \geq d - b - 2c(\Gamma)$  and, for any  $\delta > 0$ ,  $D(f) \cap \Delta_{2c(\Gamma)+\delta} \subset \Gamma^{-1}(D(f + g) \cap \Delta_\delta)$ . Then,

$$\begin{aligned} \text{pers}_{p,\epsilon}^p(f + g) &= \sum_{(b', d') \in D(f+g)} w_\epsilon(b', d')^p \\ &\geq \sum_{(b', d') \in D(f+g) \cap \Delta_\delta} w_\epsilon(b', d')^p \\ &\geq \sum_{(b, d) \in \Gamma^{-1}(D(f+g) \cap \Delta_\delta)} w_\epsilon((b, d) - c(\Gamma)(-1, 1))^p \\ &\geq \sum_{(b, d) \in D(f) \cap \Delta_{2c(\Gamma)+\delta}} w_{\epsilon+2c(\Gamma)}(b, d)^p. \end{aligned}$$

For  $\delta = \epsilon$ , the last quantity is equal to  $\text{pers}_{p,\epsilon+2c(\Gamma)}^p(f)$ . By taking the infimum over all matchings  $\Gamma$ , we obtain  $\text{pers}_{p,\epsilon}^p(f + g) \geq \text{pers}_{p,\epsilon+2\|g\|_\infty}^p(f)$ .

For the upper-bound, we first note that when  $A_f \leq \epsilon$ , then  $\text{pers}_{p,\epsilon}^p(f) = 0$ . For the non-trivial case, we follow the proof of Theorem 4.13 in [Perez \(2022\)](#). An upper-bound of the covering number of the image of  $f$ , at radius  $\tau > 0$  is  $T(2\Lambda/\tau)^{1/\alpha} + 1$ , so that

$$\begin{aligned} \text{pers}_{p,\epsilon}^p(f) &\leq p \int_\epsilon^{A(f)} \left( T \left( \frac{2\Lambda}{\tau} \right)^{1/\alpha} + 1 \right) (\tau - \epsilon)^{p-1} d\tau \\ &= (A_f - \epsilon)^p + pT(2\Lambda)^{1/\alpha} \int_\epsilon^{A(f)} \frac{(\tau - \epsilon)^{p-1}}{\tau^{1/\alpha}} d\tau. \end{aligned}$$

We recall that since  $A_f/\tau \geq 1$  and  $1/\alpha \leq p-1$ ,  $(A_f/\tau)^{1/\alpha} \leq (A_f/\tau)^{p-1}$ , so

$$\frac{(\tau - \epsilon)^{p-1}}{\tau^{1/\alpha}} = \frac{1}{A_f^{1/\alpha}} \left( \frac{A_f}{\tau} \right)^{1/\alpha} (\tau - \epsilon)^{p-1} \leq A_f^{p-1-1/\alpha} \left( 1 - \frac{\epsilon}{\tau} \right)^{p-1}.$$

Finally, by recognizing that  $1 - \epsilon/\tau \leq 1 - \epsilon/A_f$ , we obtain

$$\begin{aligned} \text{pers}_{p,\epsilon}^p(f) &\leq (A_f - \epsilon)^p + pT(2\Lambda)^{1/\alpha} A_f^{p-1-1/\alpha} (1 - \epsilon/A_f)^{p-1} (A_f - \epsilon) \\ &\leq (A_f - \epsilon)(1 - \epsilon/A_f)^{p-1} [A_f^{p-1} + pT(2\Lambda)^{1/\alpha} A_f^{p-1-1/\alpha}] \\ &\leq (A_f - \epsilon)^p \left( 1 + pT \left( \frac{2\Lambda}{A_f} \right)^{1/\alpha} \right) \\ &\leq (A_f - \epsilon)^p \left( 1 + pT \left( \frac{2\Lambda}{\epsilon} \right)^{1/\alpha} \right), \end{aligned}$$

where we have used that  $\epsilon^{1/\alpha} \leq A_f^{1/\alpha}$ .  $\square$

**Proposition 2.4 (Continuity of  $\epsilon$ -truncated  $p$ -persistence).** *For any  $\epsilon > 0$ , the total  $\epsilon$ -truncated  $p$ -persistence  $\text{pers}_{p,\epsilon}^p : C([0, T], \mathbb{R}) \rightarrow \mathbb{R}$  is continuous. In addition,  $\text{pers}_{p,\epsilon}^p$  is Lipschitz over Hölder functions: for any two  $\alpha$ -Hölder functions  $f, g$  with constant  $\Lambda$  and such that  $p - 2 > 1/\alpha$ ,*

$$\begin{aligned} |\text{pers}_{p,\epsilon}^p(f) - \text{pers}_{p,\epsilon}^p(g)| &\leq p \|f - g\|_\infty \left( \text{pers}_{p-1,\epsilon}^{p-1}(f) + \text{pers}_{p-1,\epsilon}^{p-1}(g) \right) \\ &\leq C_{p-1,\Lambda,\alpha,T} \|f - g\|_\infty. \end{aligned}$$

As for the proof of Proposition 2.3, the proof of Proposition 2.4 relies on bounds on the maximal number of oscillations of size at least  $\epsilon$ .

**Proof.** Let  $f, g \in C([0, T])$  such that  $\|f - g\|_\infty < \epsilon/4$ . Let  $\Gamma : D(f) \rightarrow D(g)$  be a matching. Recall that  $|w_\epsilon(b, d) - w_\epsilon(\eta_b, \eta_d)| \leq |b - \eta_b| + |d - \eta_d| \leq 2\|(b, d) - (\eta_b, \eta_d)\|_\infty$ . In addition, if  $d - b < \epsilon/2$ , then both  $w_\epsilon(b, d) = 0 = w_\epsilon(\Gamma(b, d))$ . Using the technique  $|x_2^p - x_1^p| = |p \int_{x_1}^{x_2} t^{p-1} dt| \leq p|x_2 - x_1| \max(x_1^{p-1}, x_2^{p-1})$  from the proof of Cohen-Steiner et al. (2010, Total Persistence Stability Theorem), we have

$$\begin{aligned} \left| \sum_{(b,d) \in D(f)} w_\epsilon(b, d)^p - \sum_{(b',d') \in D(g)} w_\epsilon(b', d')^p \right| &\leq p \sum_{(b,d) \in D(f)} |w_\epsilon(b, d) - w_\epsilon(\Gamma(b, d))| \max_{x \in \{(b,d), \Gamma(b,d)\}} w_\epsilon(x)^{p-1} \\ &\leq 2p \|f - g\|_\infty \sum_{\substack{(b,d) \in D(f) \\ d-b \geq \epsilon/2}} \max_{x \in \{(b,d), \Gamma(b,d)\}} w_\epsilon(x)^{p-1} \\ &\leq p \|f - g\|_\infty \sum_{\substack{(b,d) \in D(f) \\ d-b \geq \epsilon/2}} (w_\epsilon(b, d) + 2\epsilon/4)^{p-1} \\ &= p C_f \|f - g\|_\infty. \end{aligned}$$

Since  $f$  is continuous on a compact domain, it is uniformly continuous, so that  $C_f$  is finite and does not depend on  $g$ .

For the Lipschitz character, we follow the proof of Perez (2022, Lemma 3.20). For two  $\alpha$ -Hölder functions  $f, g$  with constant  $\Lambda$ ,

$$\left| \sum_{(b,d) \in D(f)} w_\epsilon(b, d)^p - \sum_{(b',d') \in D(g)} w_\epsilon(b', d')^p \right| \leq p \sum_{(b,d) \in D(f)} |w_\epsilon(b, d) - w_\epsilon(\Gamma(b, d))| \max_{x \in \{(b,d), \Gamma(b,d)\}} w_\epsilon(x)^{p-1}$$

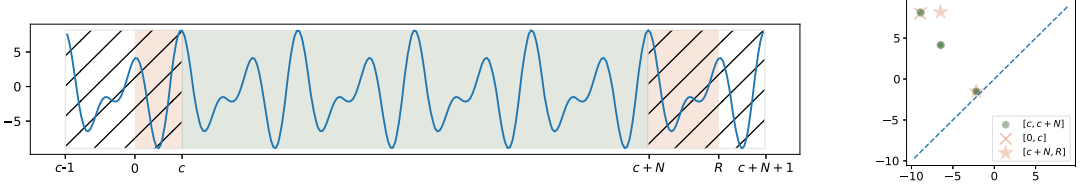


**Figure 3.** On the left, a graph with of several periods of a periodic function, observed on  $[0, R]$  for  $R = 5$ . The diagram  $D_1$  appears 4 times, and the corresponding parts are marked in green on the graph. The red parts correspond to the remainder  $D'$ . The intervals  $[c - 1, c]$  and  $[R, c + N + 1]$  included as hatched regions are used to bound the persistence of the remainder. On the left, a graph showing  $D_1$  and  $D'$  in green and red respectively.

$$\begin{aligned} &\leq 2p \|f - g\|_\infty \left( \sum_{(b,d) \in D(f)} w_\epsilon(b,d)^{p-1} + \sum_{(b',d') \in D(g)} w_\epsilon(b',d')^{p-1} \right) \\ &= 2p (\text{pers}_{p-1,\epsilon}^{p-1}(D(f)) + \text{pers}_{p-1,\epsilon}^{p-1}(D(g))) \|f - g\|_\infty. \end{aligned}$$

By Proposition 2.3,  $\text{pers}_{p-1,\epsilon}^{p-1}(D(f)) \leq T^{\alpha(p-1)} \Lambda^{p-1} (1 + (p-1)2^{1/\alpha})$ , so that

$$|\text{pers}_{p,\epsilon}^p(D(f)) - \text{pers}_{p,\epsilon}^p(D(g))| \leq 4p T^{\alpha(p-1)} \Lambda^{p-1} (1 + (p-1)2^{1/\alpha}) \|f - g\|_\infty. \quad \square$$

We now focus on the case of periodic function, for which the structure of a persistence diagram can be characterized more finely. Consider  $\phi : \mathbb{R} \rightarrow \mathbb{R}$  a 1-periodic and continuous function. We denote by  $\phi|_A$  the restriction of  $\phi$  to  $A \subset \mathbb{R}$  and by  $D \sqcup D'$  the union of two multisets. For  $n \in \mathbb{N}^*$ ,  $nD$  is the multiset with the same support as  $D$  and with multiplicities increased by a factor of  $n$ .

**Lemma 2.5 (Additivity of diagrams).** *Let  $R > 1$ . There exists  $c \in [0, 1[$  such that*

$$D(\phi|_{[0,R]}) = \left( \bigsqcup_{k=1}^{\lfloor R-1 \rfloor} D(\phi|_{[c+k-1, c+k]}) \right) \sqcup D', \quad (2)$$

for some persistence diagram  $D'$ . In addition,  $D_1 := D(\phi|_{[c, c+1]}) = D(\phi|_{[c+k-1, c+k]})$  for any  $k$  and  $\text{pers}_{p,\epsilon}(D') \leq 2\text{pers}_{p,\epsilon}(D_1)$  for any  $\epsilon \geq 0$ .

Before giving a complete proof, we provide an illustration of the core idea in Figure 3. By choosing  $c \in [0, 1]$  to be a global maximum of  $\phi$  and defining “the period” to be  $\phi|_{[c, c+1]}$ , we can decompose the diagram of  $\phi|_{[0,R]}$  as a sum of diagrams of individual periods. These diagrams are all equal and denoted  $D_1$ , except for the first and last periods which are not complete and constitute the residual part  $D'$ . Thus, we obtain (2). The total persistence of a diagram of an incomplete period is not greater than the persistence of a complete period, so  $\text{pers}_{p,\epsilon}(D') \leq 2\text{pers}_{p,\epsilon}(D_1)$ .

**Proof.** We start the proof by explicitly defining the terminated persistence modules, using the theory of persistence modules developed in Chazal et al. (2016). For  $t \in \mathbb{R}$ , we consider the  $t$ -sublevel set of  $h$ ,  $\mathbb{X}_t = h^{-1}([-\infty, t])$  and we define the *terminated module*

$$V_t := \begin{cases} H_0(\mathbb{X}_t), & \text{if } t < \max h \\ 0, & \text{otherwise,} \end{cases} \quad (3)$$



where  $H_0$  is the 0-dimensional singular homology. For any  $s \leq t < \max h$ , the inclusion  $\mathbb{X}_s \rightarrow \mathbb{X}_t$  induces a morphism between the singular homology groups  $\iota_s^t : V_s \rightarrow V_t$ . For  $t \geq \max h$ ,  $\iota_s^t$  is the zero morphism. We call  $\mathbb{V} = ((V_t)_{t \in \mathbb{R}}, (\iota_s^t)_{s < t \in \mathbb{R}})$  the *terminated persistence module* associated to  $h$ .

When  $\mathbb{X}$  is compact and  $h$  continuous, for any  $s < t$ , the rank of  $\iota_s^t$  is finite. This allows to define a measure on rectangles in  $\mathbb{R}^2$ : for any  $a < b < c < d \in \mathbb{R}$ ,

$$m([a, b] \times [c, d]) = \dim \left( \frac{\text{im}(\iota_b^c) \cap \ker(\iota_c^d)}{\text{im}(\iota_a^c) \cap \ker(\iota_c^d)} \right),$$

which counts the number of connected components of  $\mathbb{X}_b$  that appeared later than in  $\mathbb{X}_a$  and persist in  $\mathbb{X}_c$ , but not until  $\mathbb{X}_d$ . Finally, we can define the multiplicity of a point  $(s, t) \in \mathbb{R}^2$  with  $s < t$ , as  $m(s, t) = \lim_{\delta \rightarrow 0^+} m([s - \delta, s + \delta] \times [t - \delta, t + \delta])$ . The diagram  $D(h)$  is then the set of points for which the multiplicity is positive. By convention,  $m(s, s) = \infty$ , for any point  $(s, s) \in \Delta := \{(t, t) \in \mathbb{R}\}$ .

Having introduced the algebraic tools, we can now characterize the structure of the terminated persistence module of  $\phi|_{[0, R]}$ . Let  $M := \max \phi$ ,  $c := \inf\{x \in [0, 1] \mid \phi(x) = M\}$  and  $N = \max\{n \in \mathbb{N} \mid c + n \leq R\}$ . Consider the persistence modules defined by (3) for  $\phi|_{[0, c]}$ ,  $\phi|_{[c, c+N]}$  and  $\phi|_{[c+N, R]}$ . For  $t < M$ ,

$$\phi|_{[0, c]}^{-1}([-\infty, t]) \cap \phi|_{[c, c+N]}^{-1}([-\infty, t]) \subset \{c\},$$

and  $\phi(c) = M$ , so the intersection is empty and the same holds for  $\phi|_{[c+N, R]}$  and  $\phi|_{[c, c+N]}$ . Therefore,

$$\begin{aligned} H_0(\phi|_{[0, R]}^{-1}([-\infty, t])) &\simeq H_0(\phi|_{[0, c]}^{-1}([-\infty, t])) \oplus H_0(\phi|_{[c, c+N]}^{-1}([-\infty, t])) \\ &\oplus H_0(\phi|_{[c+N, R]}^{-1}([-\infty, t])). \end{aligned} \quad (4)$$

Since the isomorphism is induced by inclusions, it is an isomorphism between the persistence modules restricted to  $t \in ]-\infty, M[$ . By definition (3), the persistence modules are all 0 for  $t \geq M$ , so both sides of (4) are trivially isomorphic for  $t \geq M$ . Therefore, the persistence modules (on  $t \in \mathbb{R}$ ) are isomorphic.

By repeating the same argument as above, we can show that the persistence module of  $\phi|_{[c, c+N]}$  is the direct sum of the persistence modules of  $(\phi|_{[c+n, c+n+1]})_{n=0}^{N-1}$ . Then, for any  $n = 0, \dots, N-1$ ,  $g_n : x \mapsto x + n$  is an isomorphism between the sub level set of  $\phi|_{[c, c+1]}$  and  $\phi|_{[c+n, c+n+1]}$ , so the persistence module of  $\phi|_{[c, c+N]}$  is isomorphic to the direct sum of  $N$  copies of  $\phi|_{[c, c+1]}$ . Thus, (4) becomes

$$\begin{aligned} H_0(\phi|_{[0, R]}^{-1}([-\infty, t])) &\simeq \left( \bigoplus_{n=0}^{N-1} H_0(\phi|_{[c, c+1]}^{-1}([-\infty, t])) \right) \oplus H_0(\phi|_{[0, c]}^{-1}([-\infty, t])) \\ &\oplus H_0(\phi|_{[c+N, R]}^{-1}([-\infty, t])). \end{aligned}$$

The second crucial observation is that the diagram of a direct sum of two persistence modules is the union of diagrams. The case of interval decomposable modules is treated in Chazal et al. (2016, Proposition 2.16). The persistence modules that we consider are  $q$ -tame (Chazal et al., 2016, Theorem 3.33), so they do not necessarily admit an interval decomposition. Recall that the persistence diagram is computed via rectangle measures (Chazal et al., 2016, Section 3), defined with ranks of inclusion morphisms. For two persistence modules  $\mathbb{V} = (V_t)_{t \in \mathbb{R}}$ ,  $\mathbb{W} = (W_t)_{t \in \mathbb{R}}$  and any  $s, t \in \mathbb{R}$ , we have that  $\text{rank}((V \oplus W)_s \rightarrow (V \oplus W)_t) = \text{rank}(V_s \rightarrow V_t) + \text{rank}(W_s \rightarrow W_t)$ . This shows that the two rectangle measures  $(\mu_V + \mu_W)$  and  $\mu_{V \oplus W}$  are equal and so are their persistence diagrams. If we denote by  $D_1 := D(\phi|_{[c+n, c+n+1]})$  and by  $D'$  the diagram of the sum of the rectangle measures of the  $\phi|_{[0, c]}$  and  $\phi|_{[c+N, R]}$ , then (2) follows.

We now need to bound the  $p$ -persistence of the remainder. Denote by  $\mathbb{U}$  and  $\mathbb{V}$  the persistence modules associated to  $\phi|_{[0,c]}$  and  $\phi|_{[0,c]}$  respectively. For any  $t \in \mathbb{R}$ ,  $\phi|_{[0,c]}^{-1}(-\infty, t] \subset \phi|_{[c-1,c]}^{-1}(-\infty, t]$  induces a map  $U_t \rightarrow V_t$ . We claim that it is an injective morphism between persistence modules. Hence,  $\text{rank}(U_s \rightarrow U_t) \leq \text{rank}(V_s \rightarrow V_t)$  for any  $s < t \in \mathbb{R}$  and both are finite. Hence, to every point  $(b, d) \in D(\phi|_{[0,c]})$  with  $b < d$ , we can assign a point  $(b', d') \in D(\phi|_{[-1+c,c]})$  in such a way that this assignment is injective (considered with multiplicity) and such that  $b' \leq b < d \leq d'$ . So,  $\text{pers}_{p,\epsilon}^p(D(\phi|_{[0,c]})) \leq \text{pers}_{p,\epsilon}^p(D(\phi|_{[-1+c,c]}))$ . A similar argument shows that  $\text{pers}_{p,\epsilon}^p(D(\phi|_{[c+N,R]})) \leq \text{pers}_{p,\epsilon}^p(D(\phi|_{[c+N,c+N+1]}))$ .  $\square$

**Remark 2.6.** Usually, the persistence module associated to a continuous function is simply

$$((H_0(\mathbb{X}_t))_{t \in \mathbb{R}}, (t_s^t)_{s < t \in \mathbb{R}}).$$

We use terminated modules to force the essential component to have a finite death value, an operation particularly convenient to obtain (2).

In the case of persistence homology of sublevel sets of periodic functions, most points in the persistence diagram will have multiplicity greater than one, reflecting the number of observed periods, as stated by Lemma 2.5. When the function is corrupted by additive noise, the points will no longer be superposed. The additive structure combined with robustness in the form of the bottleneck stability motivates us to introduce normalized versions of persistence-based signatures.

## 2.2. Normalized functionals of persistence

The space of persistence diagrams is not a vector space and is ill-suited for statistical purposes. It is common to map diagrams to a functional Banach space. Many such mappings have been proposed (Adams et al., 2017, Bubenik, 2015, Carrière et al., 2020, Chung and Lawson, 2022) and their properties are described extensively. For the purpose of creating signatures of periodic functions, functionals normalized by the total persistence are of particular interest. As it is usually the case in the TDA literature, we present a general set of assumptions and we show examples of functionals from the literature (or of their adaptation) which fit within the prescribed framework.

Consider  $\mathbb{U}$  a Euclidean space and let  $\mathcal{H}$  be a Banach space of functions  $\mathbb{U} \rightarrow \mathbb{R}$ . Let  $k : \mathbb{R}^2 \rightarrow \mathcal{H}$  be a map, which to a point  $(b, d)$  in the plane associates a function  $k(b, d) : \mathbb{U} \rightarrow \mathbb{R}$ . We give two examples, the persistence silhouette kernel  $\Lambda_{(b,d)}$  from Bubenik (2015) and the persistence image kernel  $k^{pi}$  from Adams et al. (2017),

$$\begin{aligned} \Lambda_{(b,d)} : \mathbb{R} &\rightarrow \mathbb{R} & k^{pi}(b,d) : \mathbb{R}^2 &\rightarrow \mathbb{R} \\ u &\mapsto \left( \frac{d-b}{2} - |u - \frac{b+d}{2}| \right)_+, & (x,y) &\mapsto \frac{1}{2\pi\sigma^2} \exp\left( -\frac{(b-x)^2 + (d-y)^2}{2\sigma^2} \right). \end{aligned}$$

**Definition 2.7.** For a persistence diagram  $D$  with  $\text{pers}_{p,\epsilon}(D) > 0$ , the linear and the normalized functionals are defined as

$$\rho(D) := \sum_{x \in D} w_\epsilon(x)^p k(x), \quad \bar{\rho}(D) := \frac{\rho(D)}{\sum_{x \in D} w_\epsilon(x)^p}. \quad (5)$$

Otherwise, when  $\text{pers}_{p,\epsilon}(D) = 0$ , we set  $\rho(D) = 0 = \bar{\rho}(D)$ .

Note that  $\rho(D)$  and  $\bar{\rho}(D)$  are by construction elements of  $\mathcal{H}$ , that is functions from  $\mathbb{U}$  to  $\mathbb{R}$ . In this work, we are more specifically interested in diagrams of sublevel sets of functions defined on a compact interval. In this case we will abuse notation and write  $\rho(f) := \rho(D(f))$ .

**Remark 2.8.** We note a few differences with Persistence Curves introduced in [Chung and Lawson \(2022\)](#). In that article, the operator aggregating  $\{k(x)\}_{x \in D}$  is different from the sum used here. In addition, for normalized functionals, the authors only consider kernels of the form  $k(b, d)(u) = c 1_{[b, d]}(u)$ , for some  $c > 0$ , which are piecewise constant, so not continuous.

We will assume that  $k$  satisfies the following:

1.  $k(x)$  has a uniformly bounded support, for all  $x \in \mathbb{R}^2$

$$\exists K \subset \mathbb{U} \text{ compact, } k(x)|_{\mathbb{U} \setminus K} \equiv 0, \quad \forall x. \quad (6)$$

2.  $k(x)$  is Lipschitz, uniformly over  $x \in \mathbb{R}^2$

$$\exists L > 0, |k(x)(u) - k(x)(s)| \leq Ld(u, s), \quad \forall x \in \mathbb{R}^2, \forall u, s \in \mathbb{U}. \quad (7)$$

3.  $x \mapsto k(x)$  is Lipschitz

$$\exists L_k > 0, \|k(x) - k(x')\|_{\mathcal{H}} \leq L_k \|x - x'\|_{\infty}, \quad \forall x, x' \in \mathbb{R}^2. \quad (8)$$

4.  $k(x)$  is uniformly-bounded on the diagonal

$$\exists C \leq 0, \|k|_{\Delta}\|_{\mathcal{H}} \leq C. \quad (9)$$

Assumptions (7-9) are standard in the literature. Assumptions (8) and (9) guarantee that  $\|k(x)\|_{\mathcal{H}}$  is uniformly bounded on any compact subset of  $\mathbb{R}^2$ . While a condition on  $\|k(x)\|_{\mathcal{H}}$  could be imposed for a different  $x$ , an assumption for  $x \in \Delta$  is natural because points in  $\Delta$  correspond to generators in the module which exist punctually and do not persist. However, many kernels do not satisfy (6), and it is often obtained as a consequence of an assumption on the statistical model ([Berry et al., 2020](#), [Chazal et al., 2014](#)). To adapt a kernel to this assumption, we can precompose it with a projection. Specifically, let  $Q < U \in \mathbb{R}$  and consider  $\pi_{Q,U} : \Delta_{\geq 0} \rightarrow \Delta_{\geq 0}$  the operator which maps points above the diagonal, onto the upper triangle with corner at  $(Q, U)$

$$\begin{aligned} \pi_{Q,U} : \Delta_{\geq 0} &\rightarrow \Delta_{\geq 0} \\ (b, d) &\mapsto (b, d) + (1, -1) \min(\max(d - U, Q - b, 0), \frac{d-b}{2}). \end{aligned} \quad (10)$$

Examples of kernels which satisfy the assumptions (6)-(9) are given below for the Persistence Silhouette and the Persistence Image, and sample realisations are shown in Figure 4. The calculations of the Lipschitz constants are carried out in Section A of the supplement [Chazal, Michel and Reise \(2025\)](#).

**Example 2.9 (Persistence Silhouette).** We set  $k^s(b, d)(u) = \Lambda_{(\pi_{Q,U}(b, d))}(u)$ , so that

$$\text{supp}(k^s(b, d)) \subset \text{supp}(\Lambda^s(Q, U)) = [Q, U].$$

Since  $t \mapsto k^s(b, d)$  is piecewise linear with slopes 0, 1 and -1,  $L = 2 = L_k$ . The kernel is zero on the diagonal, so  $C = 0$  is enough to satisfy (9).

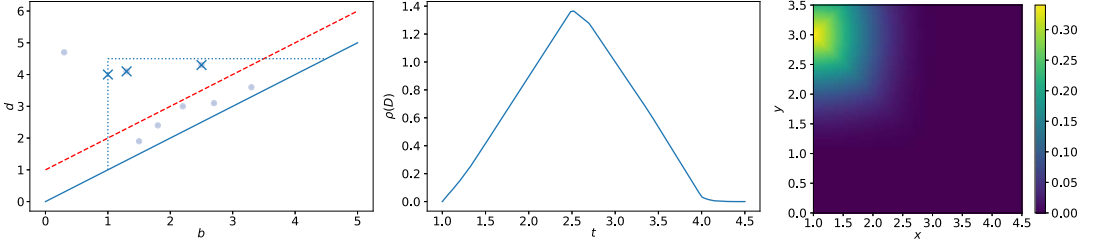


**Figure 4.** On the right, a persistence diagram with  $\epsilon = 1$ ,  $L = 1$  and  $U = 4.5$  marked in dashed and dotted lines. In the center and on the right, two functionals  $\bar{\rho}$  evaluated on that diagram, with  $k^S$  and  $k^{Pi,t}$  ( $\sigma = 1, r = 1.1$ ) respectively, both weighted by the truncated persistence  $w_\epsilon$  with  $p = 2$ .

**Example 2.10 (Persistence Image).** In order for  $k^{Pi}$  to have bounded support and remain Lipschitz, we propose to multiply by it the distance to a square of size  $2\sigma$  to  $(b, d)$ , namely, for some  $r > 1$ , set

$$k^{Pi,r}(b, d)(x, y) = \left(2 - \frac{\|\pi_{Q,U}(b, d) - (x, y)\|_\infty}{\sigma}\right)_+^r k^{Pi}(\pi_{Q,U}(b, d))(x, y).$$

We obtain the original persistence image kernel when we set  $r = 0$  and  $Q = \infty, U = \infty$ . Note that a simple truncation of  $k^{Pi}$  is not enough, as the kernel would not be continuous at the truncation interface. The function  $(x, y) \mapsto \exp(-(x^2 + y^2))$  is  $(4/e)$ -Lipschitz and  $(x, y) \mapsto (2 - \|(b, d) - (x, y)\|_\infty / \sigma)_+^r$  is  $(r2^r / \sigma)$ -Lipschitz, for the Minkowski distance. Hence,  $L_{k^{Pi,r}} = 2^{r-1}(r+2)/\pi\sigma^3$  and  $L = 2^{r+1}/\pi e\sigma^3$ .

Continuity of functionals has been studied, notably in [Divol and Polonik \(2019\)](#) and [Chung and Lawson \(2022\)](#). In the first, it was fully characterized, but only for linear functionals. In the latter, functionals were considered under the  $L^1$  metric. Due to the nature of the statistical results in [Section 3.3](#), we are particularly interested in  $\|\cdot\|_\infty$ , so we repeat the proof of [Divol and Polonik \(2019, Theorem 3\)](#) for linear functionals  $\rho$  and we derive results for normalized functionals  $\bar{\rho}$ .

**Proposition 2.11 (Stability).** *Suppose that the persistence of any point in  $D_1$  and  $D_2$  is bounded by a uniform constant  $U$  and that  $k$  satisfies (6), (8) and (9). Then,*

$$\|\rho(D_1) - \rho(D_2)\|_{\mathcal{H}} \leq \left( L_k \text{pers}_{p,\epsilon}^p(D_1) + p(L_k U + C) \sum_{k=1,2} \text{pers}_{p-1,\epsilon}^{p-1}(D_k) \right) d_B(D_1, D_2), \quad (11)$$

$$\|\bar{\rho}(D_1) - \bar{\rho}(D_2)\|_{\mathcal{H}} \leq \left( L_k + 2p(L_k U + C) \frac{\text{pers}_{p-1,\epsilon}^{p-1}(D_1) + \text{pers}_{p-1,\epsilon}^{p-1}(D_2)}{\text{pers}_{p,\epsilon}^p(D_1)} \right) d_B(D_1, D_2). \quad (12)$$

**Remark 2.12.** The result we give for  $\rho$  is a special case of [Divol and Polonik \(2019, Theorem 3\)](#). To see this, notice that using the notations of that article,  $\text{Lip}(\phi) = L_k$ ,  $A = p$ , and  $\alpha = p$ , where ‘ $p$ ’ is from our work. In their article,  $p = \infty$  and  $a = 1$ . In particular, we see exactly that  $\sup_x \|k(x)\|_{\mathcal{H}} \leq L_k U + C$ .

**Proof.** Let  $\Gamma : D_1 \rightarrow D_2$  be a matching between the two diagrams, we have

$$\|\rho(D_1) - \rho(D_2)\|_{\mathcal{H}} \leq \sum_{x \in D_1} w_\epsilon(x)^p \|k(x) - k(\Gamma(x))\|_{\mathcal{H}} + \|k(\Gamma(x))\|_{\mathcal{H}} |w_\epsilon(x)^p - w_\epsilon(\Gamma(x))^p|$$

$$\begin{aligned}
&\leq \sup_{x \in D_1} \|k(x) - k(\Gamma(x))\|_{\mathcal{H}} \sum_{x \in D_1} w_{\epsilon}(x)^p \\
&\quad + \sup_{x \in D_1} \|k(\Gamma(x))\|_{\mathcal{H}} \sum_{x \in D_1} |w_{\epsilon}(x)^p - w_{\epsilon}(\Gamma(x))^p| \\
&\leq L_k d_B(D_1, D_2) \text{pers}_{p, \epsilon}^p(D_1) \\
&\quad + p(L_k U + C) \sum_{x \in D_1} |w_{\epsilon}(x) - w_{\epsilon}(\Gamma(x))| (w_{\epsilon}(x)^{p-1} + w_{\epsilon}(\Gamma(x))^{p-1}),
\end{aligned}$$

where in the last inequality, we used that

$$\|k(\Gamma(x))\|_{\mathcal{H}} \leq L_k \|k(x_1, x_2) - k(\frac{x_1+x_2}{2}, \frac{x_1+x_2}{2})\|_{\mathcal{H}} + \|k(\frac{x_1+x_2}{2}, \frac{x_1+x_2}{2})\|_{\mathcal{H}} = L_k \frac{x_2-x_1}{2} + C.$$

The sum in the second term is bounded from above by  $d_B(D_1, D_2)(\text{pers}_{p-1, \epsilon}^{p-1}(D_1) + \text{pers}_{p-1, \epsilon}^{p-1}(D_2))$ .

Consider now the normalized version:

$$\begin{aligned}
\|\bar{\rho}(D_1) - \bar{\rho}(D_2)\|_{\mathcal{H}} &\leq \frac{\|\rho(D_1) - \rho(D_2)\|_{\mathcal{H}}}{\sum_{x \in D_1} w_{\epsilon}(x)^p} + \|\bar{\rho}(D_2)\|_{\mathcal{H}} \frac{|\sum_{x \in D_1} w_{\epsilon}(x)^p - \sum_{y \in D_2} w_{\epsilon}(y)^p|}{\sum_{x \in D_1} w_{\epsilon}(x)^p} \\
&\leq d_B(D_1, D_2) \left( L_k + p(L_k U + C) \frac{\text{pers}_{p-1, \epsilon}^{p-1}(D_1) + \text{pers}_{p-1, \epsilon}^{p-1}(D_2)}{\text{pers}_{p, \epsilon}^p(D_1)} \right) \\
&\quad + p(L_k U + C) d_B(D_1, D_2) \frac{\text{pers}_{p-1, \epsilon}^{p-1}(D_1) + \text{pers}_{p-1, \epsilon}^{p-1}(D_2)}{\text{pers}_{p, \epsilon}^p(D_1)} \\
&\leq \left( L_k + 2p(L_k U + C) \frac{\text{pers}_{p-1, \epsilon}^{p-1}(D_1) + \text{pers}_{p-1, \epsilon}^{p-1}(D_2)}{\text{pers}_{p, \epsilon}^p(D_1)} \right) d_B(D_1, D_2).
\end{aligned}$$

Combine  $\text{pers}_{p-1, \epsilon}^{p-1}(D_1) + \text{pers}_{p-1, \epsilon}^{p-1}(D_2) \leq 2 \max_{k=1,2} \text{pers}_{p-1, \epsilon}^{p-1}(D_k)$  with the observation that the bound is symmetric so that we can have  $\text{pers}_{p, \epsilon}^p(D_2)$  in the denominator.  $\square$

**Corollary 2.13.** *Let  $f \in C([0, T], \mathbb{R})$  such that  $A_f > \epsilon$ . Then, the linear and normalized functionals  $\rho(D(f))$  and  $\bar{\rho}(D(f))$  in (5) are well-defined. In addition,  $h \mapsto \bar{\rho}(D(h))$  is continuous at  $f$  for  $\|\cdot\|_{\infty}$ .*

**Proof of Corollary 2.13.** Since  $f$  is continuous on a compact domain, it is also uniformly continuous and bounded. Let  $\delta > 0$  be such that  $|f(t) - f(s)| < \epsilon$ , whenever  $|s - t| < \delta$ . By the reasoning of the proof of (Cohen-Steiner et al., 2010, Persistence Cycle Lemma),  $|\omega^{-1}([\epsilon, \infty]) \cap D(f)| \leq 1 + T/\delta$ . Let  $M_f = \max(f)$ ,  $m_f = \min(f)$ . Then,

$$\begin{aligned}
\|\rho(D(f))\|_{\mathcal{H}} &\leq \sum_{(b,d) \in D(f)} w_{\epsilon}(d-b)^p \|k(b,d)\|_{\mathcal{H}} \\
&\leq \left(\frac{T}{\delta} + 1\right) \cdot w_{\epsilon}(M_f - m_f)^p \max_{(b,d) \in D(f) \cap \Delta_{\epsilon}^+} \|k(b,d)\|_{\mathcal{H}}.
\end{aligned}$$

As stated above, the number of points is bounded from above, and so is the total persistence, thus showing that  $\rho(D(f))$  is well-defined. For the normalized functional,

$$\|\bar{\rho}(D(f))\|_{\mathcal{H}} \leq \left(\frac{T}{\delta} + 1\right) \max_{(b,d) \in D(f) \cap \Delta_{\geq \epsilon}} \|k(b,d)\|_{\mathcal{H}} \leq \left(\frac{T}{\delta} + 1\right) \max_{(b,d) \in D(f) \cap \Delta_{\geq \epsilon}} \|k(b,d)\|_{\mathcal{H}}.$$

To show the continuity, let  $z > 0$  and consider  $h \in C([0, T], \mathbb{R})$  such that  $\|f - h\|_{\infty} < r_f$ , where

$$r_f := \min \left( \frac{\text{pers}_{p-1, \epsilon}^{p-1}(f)}{4pM_f(A_f + \epsilon/2)^{p-1}}, \frac{z}{L_k + 4p(2L_k A_f) \text{pers}_{p-1, \epsilon}^{p-1}(f) / \text{pers}_{p, \epsilon}^p(f)}, \frac{A_f - \epsilon}{2} \right),$$

and  $M_f = |D(f) \cap \Delta_{\geq \epsilon/2}|$ . By continuity of truncated persistence, and with the modulus of continuity from the proof of Proposition 2.4, we have  $\text{pers}_{p-1, \epsilon}^{p-1}(h) \leq 2\text{pers}_{p-1, \epsilon}^{p-1}(f)$ . We observe that  $d - b \leq A_f$  for  $(b, d) \in D(f)$  and that  $d - b \leq A_h \leq A_f + 2\|f - h\|_{\infty} \leq 2A_f$ . Applying Proposition 2.11 to  $D_1 = D(f)$ ,  $D_2 = D(h)$  with  $U = 2A_f$ , we obtain

$$\|\bar{\rho}(D(f)) - \bar{\rho}(D(h))\|_{\mathcal{H}} \leq \left( L_k + 4p(2A_f L_k + C) \frac{\text{pers}_{p-1, \epsilon}^{p-1}(f)}{\text{pers}_{p, \epsilon}^p(f)} \right) d_B(D(f), D(h)) \leq z. \quad \square$$

### 2.3. Normalized functionals of persistence for periodic functions

Let us now go back to the persistence diagram of a 1-periodic and continuous function  $\phi : \mathbb{R} \rightarrow \mathbb{R}$ . As a consequence of the additivity of diagrams (Lemma 2.5), we find that the normalized functionals are consistent. Indeed, the functional converges because the contribution of the boundary effects in the normalized functional  $\bar{\rho}(\phi|_{[0, R]})$  decreases as the number of observed periods increases to infinity. This justifies calling the limit the “signature of  $\phi$ ”.

**Theorem 2.14 (Consistency).** *Assume that  $k$  satisfies (8) and (9). Then, there exists  $c \in [0, 1[$  such that as  $R \rightarrow \infty$ ,*

$$\bar{\rho}(D(\phi|_{[0, R]})) \xrightarrow{\|\cdot\|_{\mathcal{H}}} \bar{\rho}(D(\phi|_{[c, c+1]})).$$

**Proof.** Let  $D_1 = D(\phi|_{[c, c+1]})$ ,  $D'$  be given by Lemma 2.5 and let  $D_R = D(\phi|_{[0, R]})$ . Then,

$$\left\| \frac{\rho((R-1)D_1) + \rho(D')}{\text{pers}_{p, \epsilon}^p(D_R)} - \frac{\rho(D_1)}{\text{pers}_{p, \epsilon}^p(D_1)} \right\|_{\mathcal{H}} \leq \left\| \frac{\rho(D')}{\text{pers}_{p, \epsilon}^p(D_R)} \right\|_{\mathcal{H}} + \left\| \frac{\rho((R-1)D_1)}{\text{pers}_{p, \epsilon}^p(D_R)} - \frac{\rho(D_1)}{\text{pers}_{p, \epsilon}^p(D_1)} \right\|_{\mathcal{H}},$$

and

$$\begin{aligned} \left\| \frac{\rho((R-1)D_1)}{\text{pers}_{p, \epsilon}^p(D_R)} - \frac{\rho(D_1)}{\text{pers}_{p, \epsilon}^p(D_1)} \right\|_{\mathcal{H}} &\leq \left\| \frac{\text{pers}_{p, \epsilon}^p(D_1) \rho((R-1)D_1) - (\text{pers}_{p, \epsilon}^p((R-1)D_1) + \text{pers}_{p, \epsilon}^p(D')) \rho(D_1)}{\text{pers}_{p, \epsilon}^p(D_R) \text{pers}_{p, \epsilon}^p(D_1)} \right\|_{\mathcal{H}} \\ &\leq \frac{\|\text{pers}_{p, \epsilon}^p(D') \rho(D_1)\|_{\mathcal{H}}}{\text{pers}_{p, \epsilon}^p(D_R) \text{pers}_{p, \epsilon}^p(D_1)}, \end{aligned}$$

where we have used that for any  $N \in \mathbb{N}$ ,

$$\text{pers}_{p, \epsilon}^p(ND_1) \rho(D_1) = N \text{pers}_{p, \epsilon}^p(D_1) \rho(D_1) = \text{pers}_{p, \epsilon}^p(D_1) \rho(ND_1).$$

Now, we observe that  $\text{pers}_{p,\epsilon}^p(D_R) = \text{pers}_{p,\epsilon}^p((R-1)D_1) + \text{pers}_{p,\epsilon}^p(D') \geq (R-1)\text{pers}_{p,\epsilon}^p(D_1)$  and  $\text{pers}_{p,\epsilon}^p(D') \leq 2\text{pers}_{p,\epsilon}^p(D_1)$  to obtain that

$$\|\bar{\rho}(D(\phi|_{[0,R]})) - \bar{\rho}(D(\phi|_{[c,c+1]}))\|_{\mathcal{H}} \leq \frac{\|\rho(D')\|_{\mathcal{H}}}{\text{pers}_{p,\epsilon}^p(D_R)} + \frac{\|\text{pers}_{p,\epsilon}^p(D')\rho(D_1)\|_{\mathcal{H}}}{\text{pers}_{p,\epsilon}^p(D_R)\text{pers}_{p,\epsilon}^p(D_1)} \leq \frac{\|\rho(D')\|_{\mathcal{H}} + 2\|\rho(D_1)\|_{\mathcal{H}}}{(R-1)\text{pers}_{p,\epsilon}^p(D_1)}. \quad (13)$$

Using the Minkowski inequality,

$$\|\rho(D')\|_{\mathcal{H}} = \left\| \sum_{x \in D'} w_{\epsilon}(x)^p k(x) \right\|_{\mathcal{H}} \leq \sum_{x \in D'} |w_{\epsilon}(x)^p| \max_{x \in D'} \|k(x)\|_{\mathcal{H}} \leq \text{pers}_{p,\epsilon}^p(D') \max_{x \in D'} \|k(x)\|_{\mathcal{H}}.$$

Because  $k$  is  $L_k$ -Lipschitz by (8), for any  $x \in D'$ , we have  $\|k(x)\|_{\mathcal{H}} \leq L_k \|x - \pi(x)\|_{\infty} + \|k(\pi(x))\|_{\infty}$ , where  $\pi(b, d) = ((b+d)/2, (b+d)/2)$ . Using (9) on one hand, and the fact that the distance of any point in the diagram to  $\Delta$  is bounded by  $A_{\phi}$ , we obtain  $\|k(x)\|_{\mathcal{H}} \leq L_k A_{\phi}/2 + C$ . A similar bound holds for  $\|\rho(D_1)\|_{\mathcal{H}}$ . Going back to (13), we have that

$$\begin{aligned} \|\bar{\rho}(D(\phi|_{[0,R]})) - \bar{\rho}(D(\phi|_{[c,c+1]}))\|_{\mathcal{H}} &\leq \frac{(2|\text{pers}_{p,\epsilon}^p(D_1)| + |\text{pers}_{p,\epsilon}^p(D_1)|) \max_{x \in D'} \|k(x)\|_{\mathcal{H}}}{(R-1)\text{pers}_{p,\epsilon}^p(D_1)} \\ &\leq \frac{4(C + L_k A_{\phi})}{R-1}, \end{aligned}$$

what converges uniformly to 0 as  $R$  tends to infinity.  $\square$

We conclude the section with another stability bound of normalized functionals under reparametrization and (deterministic) additive noise.

**Proposition 2.15.** *Let  $(\gamma_k : [0, T] \rightarrow [0, R_k])_{k=1,2}$  be two fixed reparametrizations, for  $R_k > 2$  and let  $g_1, g_2 \in C([0, T], \mathbb{R})$  be two  $\alpha$ -Hölder functions with constant  $\Lambda_g$  and with sup-norm bounded as follows  $\|g_k\|_{\infty} < A_{\phi}/2$ . Then,*

$$\|\bar{\rho}(\phi \circ \gamma_1 + g_1) - \bar{\rho}(\phi \circ \gamma_2 + g_2)\|_{\mathcal{H}} \leq L_k \left( \frac{4A_{\phi}}{\min(R_1, R_2)^{-2}} + P(\max(\|g_1\|_{\infty}, \|g_2\|_{\infty})) \right),$$

where  $P(x) = O(x)$ .

The expression of  $P(x)$  can be found in the proof below. The Proposition is a straightforward consequence of Proposition 2.11 and Theorem 2.14. Note that the right-hand side is strictly positive, even in the noiseless case  $g = 0$ . It is not surprising, because the bounds we use are very crude: we remove the noise and we compare the respective signatures to the limit object  $\bar{\rho}(\phi)$ . In the next section we will provide alternative stability bounds for signatures under reparametrization and additive noise in a stochastic setting. We finish this section with the proof of Proposition 2.15, preceded by a lemma.

**Lemma 2.16 (Perturbed, pathwise version).** *Consider  $g \in C([0, T], \mathbb{R})$  an  $\alpha$ -Hölder function with constant  $\Lambda$  and set  $\delta := \|g\|_{\infty}$ . If  $2\delta \leq \max \phi - \min \phi$ , then*

$$\|\bar{\rho}(\phi + g) - \bar{\rho}(\phi)\|_{\mathcal{H}} \leq L_k (P_1 \delta + P_2 \delta^2 + P_3 \delta^3) =: L_k P(\delta),$$

where

$$P_1 = 1 + 4A_{\phi} C_T C_{p-1,p}^{\epsilon}(\phi),$$

$$P_2 = 8C_T C_{p-1,p}^\epsilon(\phi) + 4pA_\phi(C_T C_{p-2,p}^\epsilon(\phi) + \frac{C_{p-3,\Lambda,\alpha,T}}{\text{pers}_{p,\epsilon}^p(\phi)}),$$

$$P_3 = 4p \left( C_T C_{p-2,p}^\epsilon(\phi) + \frac{C_{p-3,\Lambda,\alpha,T}}{\text{pers}_{p,\epsilon}^p(\phi)} \right),$$

and

$$C_T = \frac{\lceil T \rceil}{\lceil T \rceil - 2}, \quad C_{p,p'}^\epsilon(\phi) = \frac{\text{pers}_{p,\epsilon}^p(\phi)}{\text{pers}_{p',\epsilon}^{p'}(\phi)}, \quad A_\phi = \|\phi\|_\infty.$$

**Proof.** By the diagram stability theorem,  $d_B(D(\phi + g), D(\phi)) \leq \|g\|_\infty \leq \delta$ . The persistence of a point in  $D(\phi)$  and  $D(\phi + g)$  is bounded by  $2A_\phi$  and  $2A_{\phi+g} \leq 2(A_\phi + \delta)$  respectively. Using Proposition 2.4, we also bound  $\text{pers}_{p-1,\epsilon}^p(\phi + g) \leq \text{pers}_{p-1,\epsilon}^{p-1}(\phi) + p\delta(\text{pers}_{p-2,\epsilon}^{p-2}(\phi) + \text{pers}_{p-2,\epsilon}^{p-2}(g))$ . Using the uniform bound on persistence from Proposition 2.3,  $\text{pers}_{p-2,\epsilon}^{p-2}(g) \leq C_{p-3,\Lambda,\alpha,T}$ . Finally, putting these together with Proposition 2.11, we obtain:

$$\begin{aligned} \|\bar{\rho}(\phi) - \bar{\rho}(\phi + g)\|_{\mathcal{H}} &\leq L_k \left( 1 + 2pU \frac{\text{pers}_{p-1,\epsilon}^{p-1}(\phi) + \text{pers}_{p-1,\epsilon}^{p-1}(\phi + g)}{\text{pers}_{p,\epsilon}^p(\phi)} \right) d_B(D(\phi), D(\phi + g)) \\ &\leq \delta L_k \left( 1 + 4p(\|\phi\|_\infty + \delta) \frac{2\lceil T \rceil \text{pers}_{p-1,\epsilon}^{p-1}(\phi|_{[c,c+1]}) + p\delta(\text{pers}_{p-2,\epsilon}^{p-2}(\phi) + C_{p-3,\Lambda,\alpha,T})}{(\lceil T \rceil - 2)\text{pers}_{p,\epsilon}^p(\phi)} \right) \\ &\leq \delta L_k \left[ \left( 1 + 4A_\phi C_T C_{p-1,p}^\epsilon(\phi) \right) + \right. \\ &\quad \left( 8C_T C_{p-1,p}^\epsilon(\phi) + 4pA_\phi(C_T C_{p-2,p}^\epsilon(\phi) + \frac{C_{p-3,\Lambda,\alpha,T}}{\text{pers}_{p,\epsilon}^p(\phi)}) \right) \delta^1 + \\ &\quad \left. 4p \left( C_T C_{p-2,p}^\epsilon(\phi) + \frac{C_{p-3,\Lambda,\alpha,T}}{\text{pers}_{p,\epsilon}^p(\phi)} \right) \delta^2 \right]. \end{aligned}$$

□

**Proof of Proposition 2.15.** Combining Lemma 2.16 and Theorem 2.14,

$$\begin{aligned} \|\bar{\rho}(\phi \circ \gamma_1 + g_1) - \bar{\rho}(\phi \circ \gamma_2 + g_2)\|_{\mathcal{H}} &\leq \|\bar{\rho}(\phi + (g_1)_{\gamma_1^{-1}}) - \bar{\rho}(\phi|_{[0,R_1]})\|_{\mathcal{H}} + \\ &\quad \|\bar{\rho}(\phi|_{[0,R_1]}) - \bar{\rho}(\phi|_{[0,R_2]})\|_{\mathcal{H}} + \\ &\quad \|\bar{\rho}(\phi|_{[0,R_2]}) - \bar{\rho}(\phi + (g_2)_{\gamma_2^{-2}})\|_{\mathcal{H}} \\ &\leq L_k(P(\delta_1) + P(\delta_2) + 2\frac{\frac{4}{\min(R_1,R_2)}}{\frac{4}{\min(R_1,R_2)}} \|\bar{\rho}(\phi|_{[c,c+1]})\|_{\mathcal{H}}) \\ &\leq L_k \left( P(\delta_1) + P(\delta_2) + \frac{8}{\min(R_1,R_2)-2} \frac{A_\phi}{2} \right) \\ &\leq L_k \left( P(\max(\delta_1, \delta_2)) + \frac{4A_\phi}{\min(R_1,R_2)-2} \right). \end{aligned}$$

□

### 3. Signatures of periodic signals with phase variation

In this Section we define what we call the signature of a reparametrized periodic function, in a probabilistic model. Next we provide robustness properties of the signature and statistical guarantees for its estimation.



### 3.1. Generative model and persistence-based signature

As the signature will be defined in term of an expectation, we first need to specify the probabilistic model associated to our main model (1).

- We fix  $\phi : \mathbb{R} \rightarrow \mathbb{R}$  to be a continuous and 1-periodic function.
- We consider reparametrizations which have a lower-bound on the modulus of continuity. Specifically, let  $\Gamma_{v_{\min}} := \{\gamma \in C([0, T], \mathbb{R}) \mid \gamma(s) - \gamma(t) \geq v_{\min}(s - t), \text{ for all } s \geq t\}$  be the space of reparametrizations, equipped with the Borel  $\sigma$ -algebra  $\mathcal{B}(\|\cdot\|_{\infty})$  and let  $\mu$  be a probability measure on that space.
- We consider  $C_{A_{\phi} - (\epsilon + q)}([0, T], \mathbb{R}) := \{W \in C([0, T], \mathbb{R}) \mid A_W \leq A_{\phi} - (\epsilon + q)\}$  the closed subspace of continuous functions with amplitude bounded by  $A_{\phi} - (\epsilon + q)$  for some  $q > 0$  and let  $\nu$  be a probability measure on  $(C_{A_{\phi} - (\epsilon + q)}([0, T], \mathbb{R}), \mathcal{B}(\|\cdot\|_{\infty}))$ .

Under these assumptions, we consider the stochastic process

$$S : t \mapsto \phi(\gamma(t)) + W(t), \quad (14)$$

where  $\gamma$  and  $W$  are independent,  $\gamma \sim \mu$  and  $W \sim \nu$ . Moreover the process  $\gamma$  is not assumed to be observed. Indeed, it is not necessary to observe  $\gamma$  to define our persistence-based signature, which is robust to the temporal changes.

We are now in position to introduce our persistence-based signature built on the signal  $S$ . Starting from a kernel  $k$ , we define  $\bar{\rho}(S)$  as in Equation (5). For a realization  $S(w)$  of  $S$  and  $u \in \mathbb{U}$ , and we can calculate  $\bar{\rho}(S(w))(u) \in \mathbb{R}$ . Since  $A_{S(w)} \geq A_{\phi} - A_W \geq \epsilon + q$ , by Corollary 2.13,  $\bar{\rho}(S)(u)$  is a bounded real-valued random variable. We then define the signature of  $S$  point-wise as

$$F(S)(u) := \mathbb{E}[\bar{\rho}(S)(u)] = \mathbb{E}_{\gamma \sim \mu, W \sim \nu}[\bar{\rho}(\phi \circ \gamma + W)(u)], \quad (15)$$

where the expectation is taken with respect to the law of the process.

**Remark 3.1.** Note that  $T$  is fixed in our setting, so that the ‘time’ of the observation is the same, but  $\gamma(T) - \gamma(0)$ , the number of periods of  $\phi$  in  $S$  may vary. This is in contrast with typical assumptions for functions with phase variation, where  $\gamma(T) - \gamma(0)$  is shared between observations.

We now show that  $\bar{\rho}(S) \in C(\mathbb{U}, \mathbb{R})$  is also a random process.

**Proposition 3.2.** *Under Model (14), if  $\bar{\rho} : C_{\epsilon+q}([0, T], \mathbb{R}) \rightarrow C(\mathbb{U}, \mathbb{R})$  is continuous and  $C(\mathbb{U}, \mathbb{R})$  is  $\|\cdot\|_{\infty}$ -separable, then  $\bar{\rho}(S)$  is  $(C(\mathbb{U}, \mathbb{R}), \|\cdot\|_{\infty})$ -measurable.*

Since  $\bar{\rho}(\cdot)(u)$  is applied pathwise, it is not obvious under what conditions  $\bar{\rho}(S)(u)$  is a  $\mathbb{R}$ -valued random variable and it is even less whether  $\bar{\rho}(S)$  is a  $C(\mathbb{U}, \mathbb{R})$ -valued random variable. Such considerations could be circumvented by using outer probabilities (Kosorok, 2008, Radulović, 1996), but we address them in Proposition 3.2. For the proof, we will need the following lemma, see Theorem 1.1 in Pettis (1938).

**Lemma 3.3 (Pettis’ measurability theorem).** *Consider  $h : \Omega \rightarrow E$ , where  $(E, d_E)$  is a Banach space. If  $E$  is separable as a metric space and  $h$  is weakly-measurable, then  $h$  is measurable with respect to the Borel  $\sigma$ -algebra induced by  $d_E$ .*

**Proof (proposition 3.2).** First, assume that  $S$  is weakly-measurable on  $E = C([0, T], \mathbb{R})$  and that  $(C([0, T], \mathbb{R}), \|\cdot\|_\infty)$  is separable. Using lemma 3.3, we get that  $S$  is  $\sigma(\|\cdot\|_\infty)$ -measurable. Because  $\bar{\rho} : C_{\epsilon+q}([0, T], \mathbb{R}) \rightarrow C(\mathbb{U}, \mathbb{R})$  is continuous, it is measurable for the two  $\sigma$ -algebra on the domain and co-domain. This allows us to conclude that  $\bar{\rho}(S)$  is  $(C(\mathbb{U}, \mathbb{R}), \sigma(\|\cdot\|_\infty))$ -measurable.

Let us now verify the assumptions of Lemma 3.3. We introduce the notation for the measurable spaces on which  $\gamma$  and  $W$  are defined,

$$\gamma : (\Omega_r, \mathcal{A}_r) \rightarrow (\Gamma_{v_{\min}}, \sigma(\|\cdot\|_\infty)), \quad W : (\Omega_n, \mathcal{A}_n) \rightarrow \left( C_{A_\phi - (\epsilon+q)}([0, T], \mathbb{R}), \sigma(\mathbb{R}^{[0, T]}) \right).$$

By continuity of  $\phi$ , the composition  $\phi \circ \gamma$  is  $\sigma(\mathbb{R}^{[0, T]})$ -measurable. As a sum of two (independent) random variables,  $S = \phi \circ \gamma + W$  is  $\sigma(\mathbb{R}^{[0, T]})$ -measurable for  $(\Omega, \mathcal{A})$ , where  $\Omega = \Omega_r \times \Omega_n$  and  $\mathcal{A} = \mathcal{A}_r \otimes \mathcal{A}_n$ . The product  $\sigma$ -algebra  $\sigma(\mathbb{R}^{[0, T]})$  coincides with that of weak measurability on  $\mathbb{R}^{[0, T]}$ . The space  $C([0, T], \mathbb{R})$  with the topology induced by  $\|f\|_\infty := \sup_{x \in [0, T]} |f(x)|$  is a Banach, separable space. Any subspace of a separable metric space is separable, so  $S(\Omega)$  is also separable.  $\square$

### 3.2. Robustness of the signature to reparametrization

We now investigate the robustness properties of the signature  $F$ , in both the noiseless and the additive noise settings.

#### 3.2.1. Robustness in the noiseless setting

We first consider the noiseless case  $W = 0$ . Lemma 2.1 implies that the functional depends only on the number of periods. As a consequence, the signature  $F(S)$  is also robust to the distribution of reparametrizations, but only when the distributions of endpoints are equal.

Let  $\delta_t : \gamma \mapsto \gamma_t$  be the evaluation map defined on  $\Gamma_{v_{\min}}$ . We introduce  $(\delta_{0,T})_\star \mu := \mu \circ (\delta_0, \delta_T)^{-1}$  the push-forward measure on  $\mathbb{R}^2$ , which characterizes the distribution of  $(\gamma(0), \gamma(T))$ .

**Proposition 3.4.** *Consider two probability measures  $\mu_1, \mu_2$  on  $\Gamma_{v_{\min}}$ . If we let  $\gamma_k \sim \mu_k$  such that  $(\delta_{0,T})_\star \mu_1 \stackrel{f}{=} (\delta_{0,T})_\star \mu_2$ , then*

$$F(\phi \circ \gamma_1) = F(\phi \circ \gamma_2). \quad (16)$$

**Proof.** We first show that we can condition the measure  $\mu_k$  on  $(\gamma_k(0), \gamma_k(T)) = x$ . The space of continuous functions  $C([0, T], \mathbb{R})$  is Polish, and so is  $\Gamma_{v_{\min}}$  as a closed subspace. By Bogachev (2007, Corollary 10.4.6), there are regular conditional measures  $((\mu_1)_x(d\gamma))_{x \in \mathbb{R}^2}$  and  $((\mu_2)_x(d\gamma))_{x \in \mathbb{R}^2}$ . Lemma 2.1 implies that  $\gamma \mapsto \bar{\rho}(\phi \circ \gamma)(u)$  is constant on  $\delta_{0,T}^{-1}(x)$ , for any  $x = (s, r) \in \mathbb{R}^2$ . For any  $u \in \mathbb{U}$ , using the regular conditional measure property Bogachev (2007, Definition 10.4.1),

$$\begin{aligned} F(\phi \circ \gamma_1)(u) &= \int_{\Gamma} \bar{\rho}(\phi \circ \gamma)(u) \mu_1(d\gamma) \\ &= \int_{\mathbb{R}^2} \int_{\delta_{0,T}^{-1}(x)} \bar{\rho}(\phi \circ \gamma)(u) (\mu_1)_x(d\gamma) (\delta_{0,T})_\star \mu_1(dx) \\ &= \int_{\mathbb{R}^2} \int_{\delta_{0,T}^{-1}(x)} \bar{\rho}(\phi \circ \gamma)(u) (\mu_2)_x(d\gamma) (\delta_{0,T})_\star \mu_2(dx) \\ &= F(\phi \circ \gamma_2)(u). \end{aligned} \quad \square$$

While it is disappointing to require equality of the marginals  $(\delta_{0,T})_\star \mu_1$  and  $(\delta_{0,T})_\star \mu_2$  in Proposition 3.4, removing this assumption poses a difficulty which we now discuss. In short, the main problem lies in obtaining a fine control on the persistence diagram when ‘cutting’ a domain,  $[0, R]$ , into  $[0, R_1]$  and  $[R_1, R_2]$ , for any  $0 < R_1 < R_2$ . Specifically, we need to consider the difference between  $D(\phi|_{[0, R_2]})$  and  $D(\phi|_{[0, R_1]}) \cup D(\phi|_{[R_1, R_2]})$ , and it is not zero unless  $R_1 \in \operatorname{argmax} \phi$ . When  $R_1$  is a global maximum of  $\phi$ , we can reason as in the proof of Lemma 2.5. However, this is far from the general situation, in which case the cut at  $R_1$  might induce some spurious points in the diagram, as we now illustrate and discuss briefly.

Assume for simplicity that  $\gamma_1$  and  $\gamma_2$  are fixed with  $R_k := \gamma_k(T)$ . Without loss of generality, assume that  $R_1 < R_2$  and let  $T_1 := \gamma_2^{-1}(R_1)$ . Lemma 2.1 implies that  $\bar{\rho}(\phi \circ \gamma_1) = \bar{\rho}((\phi \circ \gamma_2)|_{[0, T_1]})$ . If we let  $D_1 = D((\phi \circ \gamma_2)|_{[0, T_1]})$  and  $D_2 = D((\phi \circ \gamma_2)|_{[T_1, T]})$ , we obtain that

$$\|\bar{\rho}(\phi \circ \gamma_1) - \bar{\rho}(\phi \circ \gamma_2)\|_{\mathcal{H}} \leq \|\bar{\rho}(D_1) - \bar{\rho}(D_1 \sqcup D_2)\|_{\mathcal{H}} + \|\bar{\rho}(D_1 \sqcup D_2) - \bar{\rho}(\phi \circ \gamma_2)\|_{\mathcal{H}}. \quad (17)$$

We can conveniently analyze the first term of (17) by observing that a normalized functional of a union of diagrams is a weighted average of the normalized functionals of the individual diagrams

$$\bar{\rho}(D_1 \sqcup D_2) = \bar{\rho}(D_1) \frac{\operatorname{pers}_{p, \epsilon}^p(D_1)}{\operatorname{pers}_{p, \epsilon}^p(D_1 \sqcup D_2)} + \bar{\rho}(D_2) \frac{\operatorname{pers}_{p, \epsilon}^p(D_2)}{\operatorname{pers}_{p, \epsilon}^p(D_1 \sqcup D_2)},$$

so that

$$\begin{aligned} \|\bar{\rho}(D_1) - \bar{\rho}(D_1 \sqcup D_2)\|_{\mathcal{H}} &= \|\bar{\rho}(D_1) \left( \frac{\operatorname{pers}_{p, \epsilon}^p(D_1)}{\operatorname{pers}_{p, \epsilon}^p(D_1 \sqcup D_2)} - 1 \right) + \bar{\rho}(D_2) \frac{\operatorname{pers}_{p, \epsilon}^p(D_2)}{\operatorname{pers}_{p, \epsilon}^p(D_1 \sqcup D_2)}\|_{\mathcal{H}} \\ &= \|\bar{\rho}(D_1) - \bar{\rho}(D_2)\|_{\mathcal{H}} \frac{\operatorname{pers}_{p, \epsilon}^p(D_2)}{\operatorname{pers}_{p, \epsilon}^p(D_1 \sqcup D_2)} \\ &\leq (L_k A_\phi + C) \frac{\operatorname{pers}_{p, \epsilon}^p(D_2)}{\operatorname{pers}_{p, \epsilon}^p(D_1 \sqcup D_2)}. \end{aligned}$$

We claim that if  $\phi$  is regular enough and  $R_2 - R_1$  is small, then so is  $\operatorname{pers}_{p, \epsilon}^p(D_2)$ . The first term in (17) is thus not too problematic. On the contrary, controlling the second term in (17) is harder. Thanks to Proposition 2.11, it can be upper bounded by  $d_B(D_1 \sqcup D_2, D(\phi \circ \gamma_2))$ , which, unless  $R_1$  is a global maximum of  $\phi$ , is positive. In conclusion, we see that to get a general stability from (17), we are lacking a tight control of  $d_B(D_1 \sqcup D_2, D(\phi \circ \gamma_2))$ .

### 3.2.2. Robustness in the additive noise setting

Let us go back to the model with noise, introduced in (14). Theorem 3.5 expresses the stability of the signature for different distributions of  $\gamma$  with endpoints  $\gamma(0) = 0, \gamma(T) = R$  fixed across all reparametrizations. The aim here is to compare the impact of noise on the signature for two different parameterizations. Let  $0 < T, T v_{\min} < R$  and consider

$$\Gamma_{T, R, v_{\min}} := \{\gamma \in C([0, T], [0, R]) \mid \gamma(0) = 0, \gamma(T) = R, 0 \leq v_{\min}(t - s) \leq \gamma(t) - \gamma(s), \forall s \leq t\}.$$

The set  $\Gamma_{T, R, v_{\min}}$  is convex. It is also included in  $C([0, T], \mathbb{R})$ , so it can be naturally endowed with the sup-norm, for which it is a closed, complete and separable space. In particular, it is a Radon space, so that all measures on  $(\Gamma_{T, R, v_{\min}}, \mathcal{B}(\Gamma_{T, R, v_{\min}}))$  are inner-regular and locally-finite. Hence, we

can equip the space of probability measures on  $(\Gamma_{T,R,v_{\min}}, \mathcal{B}(\Gamma_{T,R,v_{\min}}))$  with the Wasserstein distance  $W_{1,\|\cdot\|_\infty}$  (Panaretos and Zemel, 2020).

Concerning the noise  $W$ , in addition to the bound on  $A_W$  introduced in (14), we impose a path-wise regularity condition: for some  $0 < r_1 < r_2$ ,

$$\text{there exists } K = K_{r_2,r_1}, \text{ such that } \mathbb{E}[|W_t - W_s|^{r_2}] \leq K_{r_2,r_1} |t - s|^{1+r_1}, \text{ for all } s, t \in [0, T]. \quad (18)$$

**Theorem 3.5 (Stability).** *Let  $\mu_1, \mu_2$  be two probability measures on  $\Gamma_{T,R,v_{\min}}$  and let  $\gamma_k \sim \mu_k$ , for  $k = 1, 2$ . We take the same noise process  $W$  according to Model (14) in both cases:  $W \sim \nu$  and  $W$  is independent from  $\gamma_1$  and from  $\gamma_2$ . For the normalized functional  $\bar{\rho}$  defined in (5) with a kernel  $k$  that satisfies (6, 8, 9), if  $p \geq 1 + \max(r_2, r_2/(r_1 - 1))$ , then*

$$\|F(\phi \circ \gamma_1 + W) - F(\phi \circ \gamma_2 + W)\|_{\mathcal{H}} \leq \frac{\tilde{C}(K_{r_2,r_1})}{v_{\min}^\alpha} W_{1,\|\cdot\|_\infty}(\mu_1, \mu_2)^\alpha,$$

where  $\tilde{C}(x) = O(x^{1/r_2}(1 + x^{1/(r_1-1)}))$  depends on  $\phi, \epsilon, p, q$  and  $k$ .

**Remark 3.6.** Proposition 1.11 in Azaïs and Wschebor (2009) shows that if  $W$  satisfies (18), then  $W$  has a version with  $\alpha$ -Hölder continuous sample paths, for any  $0 < \alpha < r_1/r_2$ . Difficulties in treating  $W$  come both from controlling its amplitude and the regularity. The tools that we use are sensitive to many, small fluctuations. Condition (18) allows us to control the regularity, without imposing a uniform Hölder character on all paths.

Before giving the proof, we discuss two cases showing that the control in Theorem 3.5 is satisfactory. First, suppose that  $\mu_k = \delta_{\gamma_k}$  for  $k = 1, 2$ , for some fixed  $\gamma_1, \gamma_2 \in \Gamma_{T,R,v_{\min}}$ . Then, we obtain that the signature is Hölder, with respect to the distance  $\|\gamma_1 - \gamma_2\|_\infty$ . It is expected that we do not have complete invariance: for a fixed path  $W$ , the reparametrization  $\gamma$  can influence how the points in the persistence diagram are displaced. Consider now the case of vanishing noise. If  $K_{r_2,r_1}$  decreases to zero, then so does the Hölder constant  $\Lambda_W$  and we have indeed that the right-hand side becomes zero.

Note that controlling  $\|W\|_\infty$  is not sufficient for the stability. When  $A_W < \epsilon$ , the constant factor in  $\tilde{C}(x)$  is  $C_{\Lambda_W} = L_k(1 + 8p^2 A_\phi(A_\phi - \epsilon) \text{pers}_{p-2,\epsilon}^{p-2}(\phi)/(R-2)q^p)$ . We can take the truncation parameter  $\epsilon$  small, in which case  $q \approx (A_\phi - \epsilon)$  and so, for a function with a single maximum and minimum, we have  $C_{\Lambda_W} \approx L_k(1 + 8p^2) > 0$ , which is not zero. Even though the amplitude of the noise is smaller than the cut-off  $\epsilon$ , it still has an influence on the signature. Therefore, it is important that as the amplitude decreases, the noise does not become increasingly irregular: it is the case of  $aW$ , with  $a \rightarrow 0^+$ . The almost-sure bound on  $A_W$  gives us the lower-bound on  $\text{pers}_{p,\epsilon}^P(\phi \circ \gamma + W)$ , which appears in the denominator of  $\bar{\rho}$ .

For processes of decreasing amplitude but increasingly irregular, it is more advantageous to bound  $\|W_{\gamma_1^{-1}} - W_{\gamma_2^{-1}}\|_\infty \leq 2\|W\|_\infty$  in the proof. In such a scenario however, we ignore the reparametrizations so the distance  $\|\gamma_1^{-1} - \gamma_2^{-1}\|_\infty$  disappears from the bound. Finally, it would be interesting to extend Theorem 3.5 to  $\Gamma_{v_{\min}}$  from Proposition 3.4. In that case, we do obtain  $W_1((\mu_1)_x, (\mu_2)_x)$  for almost-all  $x \in \mathbb{R}^2$ , but it is not clear that it lower-bounds  $W_1(\mu_1, \mu_2)$ .

**Remark 3.7.** When both endpoints are fixed and common to all reparametrizations, there is no reason to normalize by the total persistence. The stability comes from the continuity of the functional, not the renormalisation. Proposition 2.11 states that linear functionals of the form  $\sum_{x \in D} w_\epsilon(x)^p k_x$  are also continuous for Hölder functions, so a statement analogue to Theorem 3.5 also holds for such functionals.

**Remark 3.8.** A similar result to Proposition 2.15 could be shown for the signature  $F$ , using the regularity assumption (18).

**Proof.** We start by treating  $S$  path-wise. Using Proposition 2.11 and the bottleneck stability of persistence diagrams,

$$\begin{aligned} \|\bar{\rho}(\phi \circ \gamma_1 + W) - \bar{\rho}(\phi \circ \gamma_2 + W)\|_{\mathcal{H}} &= \|\bar{\rho}(\phi + W_{\gamma_1^{-1}}) - \bar{\rho}(\phi + W_{\gamma_2^{-1}})\|_{\mathcal{H}} \\ &\leq L_k \left( 1 + 4pU \max_{k=1,2} \frac{\text{pers}_{p-1,\epsilon}^{p-1}(\phi + W_{\gamma_k^{-1}})}{\text{pers}_{p,\epsilon}^p(\phi + W_{\gamma_k^{-1}})} \right) \|W_{\gamma_1^{-1}} - W_{\gamma_2^{-1}}\|_{\infty}, \end{aligned} \quad (19)$$

where  $L_k$  is a regularity constant of the kernel and  $U$  is an upper-bound on the persistence of any point in both diagrams. The persistence of any point in the diagram  $D(h)$  of a function  $h$  is bounded by  $A_h$ . Hence, the persistence of a point in  $D(\phi + W)$  is bounded by  $U = A_{\phi+W} \leq A_{\phi} + A_W \leq A_{\phi} + (A_{\phi} - \epsilon - q) \leq 2A_{\phi}$ .

Next, we obtain an upper-bound of  $\max_{k=1,2} \text{pers}_{p-1,\epsilon}^{p-1}(\phi + W_{\gamma_k^{-1}}) / \text{pers}_{p,\epsilon}^p(\phi + W_{\gamma_k^{-1}})$ . By Proposition A.1, we can assume that  $W$  has  $\alpha$ -Hölder paths with a (random) constant  $\Lambda_W$ , for  $\alpha := \min(1, r_1 - 1)/r_2$ . This implies that  $1 + 1/\alpha < p$  and we use the continuity of truncated persistence from Proposition 2.4 to obtain

$$\text{pers}_{p-1,\epsilon}^{p-1}(\phi + W_{\gamma_k^{-1}}) \leq \text{pers}_{p-1,\epsilon}^{p-1}(\phi|_{[0,T]}) + (p-1)\|W\|_{\infty}(\text{pers}_{p-2,\epsilon}^{p-2}(\phi|_{[0,T]}) + \text{pers}_{p-2,\epsilon}^{p-2}(W_{\gamma_k^{-1}})). \quad (20)$$

For any  $x \in [0, 1]$  and  $p \geq 0$ , the function  $p \mapsto x^p$  is decreasing, so that

$$\begin{aligned} \text{pers}_{p-1,\epsilon}^{p-1}(\phi|_{[0,T]}) &= (A_{\phi} - \epsilon)^{p-1} \sum_{(b,d) \in D} \max\left(\frac{d-b-\epsilon}{A_{\phi}-\epsilon}, 0\right)^{p-1} \\ &\leq (A_{\phi} - \epsilon)^{p-1} \sum_{(b,d) \in D} \max\left(\frac{d-b-\epsilon}{A_{\phi}-\epsilon}, 0\right)^{p-2} \\ &= (A_{\phi} - \epsilon) \text{pers}_{p-2,\epsilon}^{p-2}(\phi). \end{aligned}$$

Since  $\|W\|_{\infty} < (A_{\phi} - \epsilon)/2$  and the persistence does not depend on the parametrization, equation (20) becomes

$$\begin{aligned} \text{pers}_{p-1,\epsilon}^{p-1}(\phi + W_{\gamma_k^{-1}}) &\leq (A_{\phi} - \epsilon) \text{pers}_{p-2,\epsilon}^{p-2}(\phi) \left( 1 + \frac{p-1}{2} \left( 1 + \frac{\text{pers}_{p-2,\epsilon}^{p-2}(W)}{\text{pers}_{p-2,\epsilon}^{p-2}(\phi)} \right) \right) \\ &\leq p(A_{\phi} - \epsilon) \text{pers}_{p-2,\epsilon}^{p-2}(\phi) \left( 1 + \frac{1}{2} \frac{\text{pers}_{p-2,\epsilon}^{p-2}(W)}{\text{pers}_{p-2,\epsilon}^{p-2}(\phi)} \right). \end{aligned}$$

An upper-bound for the persistence of  $W$  is given in Proposition 2.3

$$\text{pers}_{p,\epsilon}^p(W) \leq (A_W - \epsilon)^p \left( 1 + pT \left( \frac{2\Lambda_W}{\epsilon} \right)^{1/\alpha} \right),$$

where  $\Lambda_W$  is the path-wise Hölder constant of  $W$ . The amplitude  $A_{\phi}$  upper-bounds the persistence of a point and it is also realized as the persistence of a pair of a global minimum and a global maximum,

so  $\text{pers}_{p-2,\epsilon}^{p-2}(\phi|_{[0,R]}) \geq (R-2)(A_\phi - \epsilon)^{p-2}$  and hence

$$\frac{\text{pers}_{p,\epsilon}^p(W)}{\text{pers}_{p-2,\epsilon}^{p-2}(\phi)} \leq \left( \frac{A_W - \epsilon}{A_\phi - \epsilon} \right)^{p-2} (A_W - \epsilon)^2 \frac{T}{R-2} \left( 1 + p \left( \frac{2\Lambda_W}{\epsilon} \right)^{1/\alpha} \right).$$

Putting the above together, with  $p \geq 2$ ,

$$\begin{aligned} \text{pers}_{p-1,\epsilon}^{p-1}(\phi + W_{\gamma_k^{-1}}) &\leq p(A_\phi - \epsilon) \text{pers}_{p-2,\epsilon}^{p-2}(\phi) \\ &\quad \times \left( 1 + \left( \frac{A_W - \epsilon}{A_\phi - \epsilon} \right)^{p-2} (A_W - \epsilon)^2 \frac{T}{R-2} \max \left( 1, p \left( \frac{2\Lambda_W}{\epsilon} \right)^{1/\alpha} \right) \right). \end{aligned}$$

We have therefore an upper-bound for the numerator. To lower-bound the denominator, we use Proposition 2.3:

$$\begin{aligned} \text{pers}_{p,\epsilon}^p(\phi + W_{\gamma_k^{-1}}) &\geq \text{pers}_{p,\epsilon+A_W}^p(\phi) \\ &\geq (R-2)(A_\phi - (A_W + \epsilon))^p \\ &\geq (R-2)(A_\phi - (A_\phi - \epsilon + q + \epsilon))^p = (R-2)q^p. \end{aligned}$$

We conclude that  $C_{\Lambda_W}$  upper-bounds  $\max_k \text{pers}_{p-1,\epsilon}^{p-1}(\phi + W_{\gamma_k^{-1}}) / \text{pers}_{p,\epsilon}^p(\phi + W_{\gamma_k^{-1}})$ ,

$$\begin{aligned} C_{\Lambda_W} &:= L_k \left( 1 + \frac{8p^2 A_\phi}{(R-2)q^p} (A_\phi - \epsilon) \text{pers}_{p-2,\epsilon}^{p-2}(\phi) \right. \\ &\quad \left. \times \left( 1 + \left( \frac{A_W - \epsilon}{A_\phi - \epsilon} \right)^{p-2} (A_W - \epsilon)^2 \frac{T}{R-2} \max \left( 1, p \left( \frac{2\Lambda_W}{\epsilon} \right)^{1/\alpha} \right) \right) \right). \end{aligned}$$

As  $A_W \leq A_\phi - \epsilon - q$ , the only remaining stochastic term in  $C_{\Lambda_W}$  is  $\Lambda_W^{1/\alpha}$ . Also, the bound only depends on  $R$  (which is fixed), but not on  $\gamma$  itself.

Let  $\pi : \mathcal{A}_{r,1} \times \mathcal{A}_{r,2} \rightarrow \mathbb{R}$  be a coupling of  $\mu_1$  and  $\mu_2$ . Specifically,  $\pi$  is a measure on the product space  $(\mathcal{G} \times \mathcal{G}, \mathcal{A}_{r,1} \otimes \mathcal{A}_{r,2})$ , such that  $\pi(A, \mathcal{G}) = \mu_1(A)$  and  $\pi(\mathcal{G}, A) = \mu_2(A)$ , for all  $A \in \mathcal{A}$ . Then,  $\pi \otimes \nu : ((A_1, B_1), (A_2, B_2)) \mapsto \pi(A_1, A_2) \nu(B_1 \cap B_2)$  is a coupling of  $\mu_1 \otimes \nu$  and  $\mu_2 \otimes \nu$ . Using the coupling and (19),

$$\begin{aligned} \|\mathbb{E}[\bar{\rho}(\phi \circ \gamma_1 + W) \mid W] - \mathbb{E}[\bar{\rho}(\phi \circ \gamma_2 + W) \mid W]\|_{\mathcal{H}} &= \|\mathbb{E}_\pi[\bar{\rho}(\phi \circ \gamma_1 + W) - \bar{\rho}(\phi \circ \gamma_2 + W) \mid W]\|_{\mathcal{H}} \\ &\leq \mathbb{E}_\pi[\|\bar{\rho}(\phi \circ \gamma_1 + W) - \bar{\rho}(\phi \circ \gamma_2 + W)\|_{\mathcal{H}} \mid W] \\ &\leq C_{\Lambda_W} \mathbb{E}[\|W_{\gamma_1^{-1}} - W_{\gamma_2^{-1}}\|_\infty \mid W] \\ &\leq C_{\Lambda_W} \Lambda_W \mathbb{E}[\|\gamma_1^{-1} - \gamma_2^{-1}\|_\infty^\alpha]. \end{aligned}$$

We have thus completely separated the bound into a product, with terms depending on  $\nu$  and  $(\mu_1, \mu_2)$ .

On one hand, it remains to take the expectation with respect to  $W$ . We bound the moments of  $\Lambda_W$  using Theorem A.2, obtaining

$$\begin{aligned} \mathbb{E}[\Lambda_W] &\leq 16 \frac{\alpha+1}{\alpha} (K_{r_2, r_1})^{1/r_2}, \\ \mathbb{E}[\Lambda_W^{1+1/\alpha}] &\leq 6^{r_2+2} K_{r_2, r_1}^{(1/r_2+1/(r_1-1))}. \end{aligned}$$

On the other hand, by Jensens' inequality,  $\mathbb{E}[\|\gamma_1^{-1} - \gamma_2^{-1}\|_\infty^\alpha] \leq \mathbb{E}[\|\gamma_1^{-1} - \gamma_2^{-1}\|_\infty]^\alpha$ . Using the lower-bound on the modulus of continuity,

$$\sup_{r \in [0, R]} |\gamma_1^{-1}(r) - \gamma_2^{-1}(r)| = \sup_{t \in [0, T]} |t - \gamma_2^{-1}(\gamma_1(t))| \leq \sup_{t \in [0, T]} \frac{1}{v_{\min}} |\gamma_2(t) - \gamma_1(t)|.$$

Taking the infimum over couplings, we obtain the 1-Wasserstein distance  $W_1(\mu_1, \mu_2)$ .  $\square$

### 3.3. Estimation of the signature of a time series

We have defined the signature and studied its properties for continuous observations. In practical applications, we do not have access to  $S$ , but to observations in the form of a time series  $\mathbf{X} = (X_n)_{n=1}^N$ . The purpose of this section is to show how to exploit the periodicity mechanism to obtain asymptotic statistical guarantees for signatures of a discretized signal.

#### 3.3.1. Time series model

We now consider a time series  $(X_n)_{n \geq 1}$  which appears as a reparametrization of a 1-periodic function  $\phi$ :

$$X_n = \phi(\gamma_n) + W_n \in \mathbb{R}, \quad (21)$$

where  $(\gamma_n)_{n \geq 1}$  is a strictly increasing time series and  $(W_n)_{n \geq 1}$  is a stationary noise time series satisfying  $\mathbb{E}[W_n] = 0$  and  $|W_n| \leq (A_\phi - \epsilon - q)/2$  almost-surely. Moreover,  $(\gamma_n)_{n \geq 1}$  and  $(W_n)_{n \geq 1}$  are assumed to be independent.

We consider a class of reparametrization processes, defined as discrete integrals of another, positive time series  $(V_n)_{n \geq 1}$ . Specifically, let

$$\gamma_{n+1} = \gamma_n + hV_n = \gamma_0 + h \sum_{k=0}^n V_k, \quad (22)$$

where  $(V_n)_{n=0}^N$  is a sequence of random variables in  $I := [v_{\min}, v_{\max}] \subset ]0, \infty[$ , independent of  $\gamma_0$  and  $h > 0$  is a time step.

This model is inspired by dynamics, where the sequence  $(\gamma_n)_{n \in \mathbb{N}}$  could model the displacement of a body over time and  $V_n$  should be thought of as the instantaneous speed. As for the continuous framework studied before, the latent times  $\gamma_n$  are not assumed to be observed.

We will consider two models for  $(V_n)_{n \in \mathbb{N}}$ . In the first one, consecutive velocities are independent. Since we do not expect a moving body to change speed abruptly, we also consider  $V_n$  as a Markov process on  $I$ . In both models, we need assumptions which guarantee that the velocity does not remain fixed and that we will observe different parts of the signal. In Model 1, it is the lower-bound by the density, while in Model 2 - the lower-bound of the density directly.

**Model 1** ( $(V_n)_{n \in \mathbb{N}}$  **i.i.d.**). We assume that  $V_n$  are independent and follow the same, unknown distribution on  $\mathbb{R}_+^*$ , which satisfies the following property: there exists  $0 < a, b, c$  such that, for all  $A \in \mathcal{B}(]a, b[)$  measurable,  $P(V_k \in A) \geq c\mu(A)$ , where  $\mu$  is the Lebesgue measure.

**Model 2** ( $(V_n)_{n \in \mathbb{N}}$  **a Markov Chain**). Let  $(V_n)_n$  be a Markov Chain with transition kernel  $P$ . Specifically,  $v \mapsto P(v, A)$  is  $\mathcal{B}(I)$ -measurable for all  $A \in \mathcal{B}(I)$ , and  $A \mapsto P(v, A)$  is a probability measure on  $(I, \mathcal{B}(I))$ . We further assume that  $P(x, \cdot)$  is a probability measure that has a density  $f_x$  with respect to  $\mu$  and that:

1. the density is lower-bounded in a small neighborhood: there exists  $\eta, \mu_0 > 0$ , such that

$$f_v|_{[v-\eta, v+\eta] \cap I} \geq \mu_0, \quad (23)$$

2.  $v \mapsto f_v(x)$  is continuous for any  $x \in I$ .

Note that if  $f_x = f$ , for all  $x \in I$ , Model 2 reduces to a particular case of the i.i.d setting, where  $P$  has density  $f$ ,  $a = v_{\min}$ ,  $b = v_{\max}$  and  $c = \mu_0$ .

**Example 3.9.** Set  $V_0 \sim \mathcal{U}(I)$  and let  $0 < \eta < (v_{\max} - v_{\min})/4$ . An example of a transition kernel satisfying assumptions of Model 2 is a truncated Gaussian kernel. The truncation is such that the support is  $I$  and  $\sigma = \eta$ .

### 3.3.2. Stationary regime for Models 1 and 2

In the next section, we will introduce a topological signature for  $(X_n)_{n \geq 1}$ . To do this, we consider the stationary regime, as we assumed earlier for continuous processes. We will also discuss extensions to the non stationary setting at the end of the section. Note that  $(\gamma_n)_{n \geq 1}$  in (22) is not generally a stationary time series. For instance, for both Models 1 and 2, we have  $P(\gamma_n < \gamma_{n+1}) = 1$ .

For Model 1, the crucial observation is that the time series  $(\text{frac}(\gamma_n))_{n \geq 1}$  is stationary, where  $\text{frac}(x) := x - \lfloor x \rfloor$  denotes the fractional part of a real number. See Appendix B.1 for a formal proof. The time series  $(\phi(\gamma_n))_{n \geq 1} = (\phi(\text{frac}(\gamma_n)))_{n \geq 1}$  and  $(X_n)_{n \geq 1}$  are thus stationary.

Regarding Model 2, it can be checked that  $(\text{frac}(\gamma_n), V_n)_{n \geq 1}$  is a Markov Chain which admits a stationary measure  $\pi_2$  (see Appendix B.2 for details). Under the initial measure  $\pi_2$  the time series  $(\text{frac}(\gamma_n))_{n \geq 1}$  is thus stationary and so is  $(X_n)_{n \geq 1}$ . We will thus assume this initial measure in order to stay in the stationary setting and denote *Model 2-S* this setting.

### 3.3.3. Signature of the time series

As we did for the continuous model, we operate at a fixed time horizon. In the time series setting, we fix  $M \in \mathbb{N}$ . From the observed time series  $(X_n)_{n=1}^N$ , we define “windows”  $\mathbf{X}_n$ , each of length  $M$  along the time series by

$$\mathbf{X}_n = (X_n, \dots, X_{n+M-1}) \quad \text{for } n = 1, \dots, N - M + 1. \quad (24)$$

Each vector  $\mathbf{X}_n$  is a  $\mathbb{R}^M$ -valued random vector, and under Models 1 and 2-S, the time series  $(\mathbf{X}_n)_{n \geq 1}$  is stationary.

We want to extend the definition of the signature  $F$  to compute it on  $\mathbf{X}_n$ . Starting from a kernel  $k$ , we first extend the definition of the normalized functional  $\bar{\rho}$  to define it on a vector of length  $M$  by

$$\bar{\rho}(\mathbf{X}_1) := \bar{\rho}(\tilde{S}_M), \quad (25)$$

where  $\tilde{S}_M$  is a continuous process on  $[0, T]$  which interpolates between entries of  $\mathbf{X}_1$ . Specifically, we define  $\tilde{S}_M$  by prescribing its values on the set  $((m-1)T/(M-1), X_m)_{m=1}^M$  and linearly interpolating in between. The resulting process  $\tilde{S}_M$  follows the continuous model (14), so that  $\bar{\rho}(\tilde{S}_M)$  is well-defined. We then define the signature by integrating  $\bar{\rho}(\mathbf{X}_1)$ :

$$F_M(\mathbf{X}_1) := \mathbb{E}[\bar{\rho}(\mathbf{X}_1)].$$

Note that  $F_M(\mathbf{X}_1)$  is a function from  $\mathbb{U}$  to  $\mathbb{R}$ . Under Models 1 and 2-S, we obviously have  $F(\mathbf{X}_1) = F(\mathbf{X}_n)$  for any  $n = 1 \dots N - M + 1$ , we thus can write

$$F_M := F_M(\mathbf{X}_1) = F_M(\mathbf{X}_n).$$



We now discuss the interest of introducing this signature for the study of time series. When the discrete model (21)-(22) corresponds to discrete observations of an underlying continuous model of the form of (1), then the interpolated signal  $\tilde{S}_M$  will be close to its corresponding complete signal  $S$ , when  $\phi$  and the noise process are smooth enough. In the noiseless case, Theorem 2.14 shows that  $F(S)$  converges to  $F(\phi_{[c,c+1]})$ , which is an intrinsic signature of the underlying signal  $\phi$ , as the number of observed periods tends to infinity. To summarize, in an idealized situation where there is very little noise, for  $\mathbf{X}_1$  a dense enough sampling along the continuous signal, and for  $M$  large enough, the quantity  $F_M(\mathbf{X}_1)$  will be close to the intrinsic quantity  $F(\phi_{[c,c+1]})$  which does not depend on the parametrization. Out of the previous idealized setting, the signature  $F_M(\mathbf{X}_1)$  also depends on the noise distribution. However, the signature is robust (as justified by Theorem 3.5 in the continuous setting). This signature then can be used for standard data sciences purposes, as for instance change point detection along a periodic phenomenon subject to phase variations, and for which we wish to develop indicators robust to phase variations.

### 3.3.4. Estimation of the signature

In practice, the signature  $F_M$  has to be estimated because the expectation is unknown. The empirical counter-part of  $F_M$  is the empirical mean

$$\hat{F}_{M,N} = \frac{1}{N-M+1} \sum_{n=1}^{N-M+1} \bar{\rho}(\mathbf{X}_n),$$

where  $\bar{\rho}(\mathbf{X}_n)$  is defined according to (25). The distribution of  $\hat{F}_{M,N}$  can be estimated by Moving Block Bootstrap (MBB), see Bühlmann (2002). Indeed, the usual nonparametric bootstrap allows to estimate the distribution of the empirical mean from independent data, but the functional nature of our observations prevents us from using it. The MBB is a common technique, designed for settings with dependency. To be specific, let  $L = L(N - M + 1) \in \mathbb{N}$  be the block length and let  $B = \frac{L}{N-M+1}$  the number of blocks we now define, which, without loss of generality, is assumed to be integer-valued. The MBB consists of sampling  $B$  blocks, each composed of  $L$  consecutive vectors  $\mathbf{X}_i$ : that is,  $(\mathbf{X}_n, \dots, \mathbf{X}_{n+L-1})$ , for  $n \in \{1, \dots, N - M + 1\}$ . The MBB sample is then

$$(\mathbf{X}_1^*, \dots, \mathbf{X}_{N-M+1}^*) := (\underbrace{\mathbf{X}_{n_1}, \dots, \mathbf{X}_{n_1+L-1}}_{\text{block 1}}, \underbrace{\mathbf{X}_{n_2}, \dots, \mathbf{X}_{n_2+L-1}}_{\text{block 2}}, \dots, \underbrace{\mathbf{X}_{n_B}, \dots, \mathbf{X}_{n_B+L-1}}_{\text{block B}}),$$

where  $n_1, \dots, n_B \sim \mathcal{U}(1, \dots, N - M + 1)$  are independent. We finally define the bootstrap signature

$$\hat{F}_{M,N}^* = \frac{1}{N-M+1} \sum_{n=1}^{N-M+1} \bar{\rho}(\mathbf{X}_n^*).$$

Note that the MBB strategy is applied to the time series of vectors  $(\mathbf{X}_n)_{n=1}^{N-M+1}$ , and not to the initial time series  $(X_n)_{n=1}^N$ , see Figure 5 for an illustration. Also note that the bootstrap sample contains overlapping samples at two different levels. Not only are the windows  $\mathbf{X}_1, \dots, \mathbf{X}_N$  overlapping, but also the different blocks can overlap.

We now prove that the empirical mean  $\hat{F}_{M,N}$  converges to  $F_M$  and that we can approximate the distribution of  $\hat{F}_{M,N}$  by that of the bootstrap signature  $\hat{F}_{M,N}^*$ , as  $N \rightarrow \infty$ . The core idea resides in exploiting the periodicity to control how the dependence between  $\mathbf{X}_1$  and  $\mathbf{X}_{1+k}$  changes as  $k$  increases. For this, we recall the definition of two mixing coefficients, see for instance Doukhan (1994).

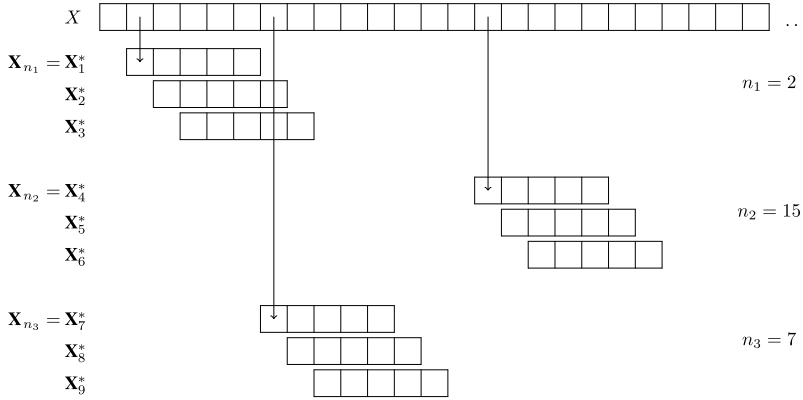


**Figure 5.** A schematic representation of the MBB, for  $M = 5$  and  $L = 3$ .

For a stationary sequence  $(Y_n)_{n \in \mathbb{N}}$  of random variables, denote by  $\sigma_{a,b}$  the  $\sigma$ -algebra generated by  $Y_a, \dots, Y_b$ . The  $k$ -th  $\phi$ -mixing coefficient is

$$\phi_Y(k) = \sup_{A \in \sigma_{-\infty,0}, B \in \sigma_{k,\infty}, P(A) > 0} |P(B|A) - P(B)|.$$

The  $k$ -th  $\beta$ -mixing coefficient is

$$\beta_Y(k) = \frac{1}{2} \sup_{\substack{\mathcal{A} \subset \sigma_{-\infty,0}, A \in \mathcal{A}, B \in \mathcal{B} \\ \mathcal{B} \subset \sigma_{k,\infty}}} \sum |P(A \cap B) - P(A)P(B)|,$$

where  $\mathcal{A}, \mathcal{B}$  are countable partitions of the sample space. We say that  $(Y_n)_{n \in \mathbb{N}}$  is *absolutely regular* (or  $\beta$ -mixing) if  $\beta_Y(k) \rightarrow 0$  as  $k \rightarrow \infty$ . A process for which  $\beta(k) \leq a^k$ , for some  $0 < a < 1$  is called *exponentially  $\beta$ -mixing*. The same definitions apply for the uniform mixing coefficients  $\phi_Y$ . Moreover we have that  $\beta_Y(k) \leq \phi_Y(k)$ .

**Theorem 3.10.** *Let the stationary time series  $(X_n)_{n \geq 1}$  defined by (22) and (24), with  $(V_n)_{n \geq 1}$  as in Model 1 or 2-S. Assume that  $(W_n)_{n \geq 1}$  is exponentially  $\beta$ -mixing. Then,*

$$\sqrt{N - M + 1}(\hat{F}_{M,N} - F_M) \rightarrow G_M \quad \text{as } N \rightarrow \infty, \quad (26)$$

where  $G_M$  is a zero-mean Gaussian process with covariance

$$(s, t) \mapsto \lim_{k \rightarrow \infty} \sum_{n=1}^{\infty} \text{cov}(\bar{\rho}(\mathbf{X}_k)(s), \bar{\rho}(\mathbf{X}_n)(t)). \quad (27)$$

In addition, if  $L(N) \rightarrow \infty$  and  $L(N) = O(N^{1/2-\epsilon})$  for some  $\epsilon > 0$ , then the bootstrap is almost surely valid:

$$\sqrt{N - M + 1}(\hat{F}_{M,N}^* - \hat{F}_{M,N}) \rightarrow^* G_M \quad \text{as } N \rightarrow \infty, \quad (28)$$

where the convergence is for the (conditional) bootstrap distribution.

This result is a functional central limit theorem, similar to many in the literature of topological data analysis, see for example [Chazal et al. \(2014\)](#) and [Berry et al. \(2020, Proposition 2 and 3\)](#), except that the samples are not independent. For independent data, it is sufficient to control the complexity of the functional family. The novel aspect of Theorem 3.10 is the consideration of dependence and it is what we treat with more care. More precisely, we show the following result:

**Proposition 3.11.** *Let the time series  $(X_n)_{n \geq 1}$  defined by (24) with  $(V_n)_{n \geq 1}$  as in (22).*

1. *If  $(V_n)_{n \geq 1}$  satisfies Model 1 then the Markov Chain  $(\text{frac}(\gamma_n))_{n \geq 1}$  is exponentially  $\phi$ -mixing.*
2. *If  $(V_n)_{n \geq 1}$  satisfies Model 2 then the Markov Chain  $(\text{frac}(\gamma_n), V_n)_{n \geq 1}$  is exponentially  $\phi$ -mixing, whatever the initial measure.*

Note that the proposition is valid for Model 2 in general, meaning also for non stationary regimes, and in that case more general definitions for  $\beta$ - and  $\phi$ -mixing coefficients are used, see for instance [Doukhan \(1994\)](#).

The complete proof of Proposition 3.11 is given in Section B of the supplement [Chazal, Michel and Reise \(2025\)](#). It relies on a general theorem for Markov chains given in [Doukhan \(1994\)](#), and which requires a Doeblin-type condition.

**Sketch of the proof of Proposition 3.11.** For Model 1, we show that a uniform measure with small but non-zero mass lower-bounds the distribution of  $\text{frac}(\sum_{k=0}^n V_k)$ . The fact that the process  $(\text{frac}(\gamma_0 + \sum_{k=0}^n V_k))_{n \in \mathbb{N}}$  is  $\phi$ -mixing then follows from general results in dependence theory ([Doukhan, 1994, Section 2.4, Theorem 1](#)). When  $V_n$  is generated using Model 2, we find a similar uniform lower-bound for the  $n$ -step transition measure of  $(\text{frac}(\gamma_n), V_n)$ . With the assumptions on the kernel in our model, we show that for  $n$  sufficiently large, this lower-bound can be taken to be a uniform measure on  $[0, 1] \times I$  with small but non-zero mass, chosen uniformly in the initial conditions  $(\text{frac}(\gamma_0), V_0)$ . We conclude again with ([Doukhan, 1994, Section 2.4, Theorem 1](#)). This concludes the proof that  $(\text{frac}(\gamma_n), V_n)_{n \in \mathbb{N}}$  is exponentially  $\phi$ -mixing.  $\square$

We now give the proof of Theorem 3.10, with all details deferred to the supplement [Chazal, Michel and Reise \(2025\)](#).

**Proof of Theorem 3.10.** The functional Central Limit Theorem we use to show Theorem 3.10 relies on the control of  $\beta$ -mixing coefficients in the stationary regime. Moreover, we know that  $\beta$ -mixing coefficients are upper bounded by  $\phi$ -mixing coefficients. Thus, under the assumptions of the theorem, we obtain from Proposition 3.11 that

- under Model 1:  $(\text{frac}(\gamma_n))_{n \geq 1}$  is exponentially  $\beta$ -mixing.
- under Model 2-S:  $(\text{frac}(\gamma_n), V_n)_{n \geq 1}$  is exponentially  $\beta$ -mixing, and thus  $(\text{frac}(\gamma_n))_{n \geq 1}$  is also exponentially  $\beta$ -mixing.

Next, we analyze how the dependence of  $(\phi(\gamma_n))_{n \in \mathbb{N}}$  and  $(W_n)_{n \in \mathbb{N}}$  shapes the dependence of  $(X_n)_{n \in \mathbb{N}}$  and that between the windows  $\mathbf{X}_1, \dots, \mathbf{X}_{N-M+1}$ . Specifically, we have the following inequality

$$\beta_{\mathbf{X}}(k) \leq \beta_X(k - (M + 1)) \leq \beta_{\text{frac}(\gamma)}(k - (M + 1)) + \beta_W(k - (M + 1)), \quad \text{for } k \geq M + 1,$$

of which we present a detailed proof in Section C of the supplement [Chazal, Michel and Reise \(2025\)](#). Since  $(W_n)_{n \in \mathbb{N}}$  is exponentially  $\beta$ -mixing by assumption,  $(\mathbf{X}_n)_{n \in \mathbb{N}}$  is exponentially  $\beta$ -mixing. The Gaussian approximation (26) is a consequence of [Kosorok \(2008, Theorem 11.24\)](#), the statement of

which is included in Appendix C. Indeed, the arguments above ensure that the mixing coefficients satisfy

$$\sum_{k=1}^{\infty} k^{\frac{2}{r-2}} \beta_{\mathbf{X}}(k) < \infty,$$

for some  $r \in ]2, \infty[$ . It remains to verify that the bracketing entropy of the functional family  $\{\bar{\rho}_u\}_{u \in \mathbb{U}}$  is controlled, see Section D in the supplement Chazal, Michel and Reise (2025). The approximation of the distribution of the empirical mean by the bootstrap distribution (28) is a consequence of Bühlmann (1995, Theorem 1), for which we only need the aforementioned results (see Appendix C).  $\square$

**Remark 3.12.** Note that length  $M$  of the window is fixed in the Theorem, it does not vary with  $N$ . It would be interesting to make this quantity increases with  $N$ . For instance, when we use this signature to compare two time series, our understanding is that increasing  $M$  may improve the discriminative power of the signature. But too large  $M$  will also decrease the sample size of windows  $\mathbb{X}_n$ , and then the variance of the empirical signature will increase. Choosing  $M$  is a non-trivial issue, which moreover cannot be easily resolved in practice by a cross-validation approach.

**Remark 3.13.** A classical framework in Functional Data Analysis (FDA) is when we have access to a collection of  $K$  time series from the same model. Many contributions have been proposed to study this statistical setting, see for instance Ramsay and Silverman (2002). To recast our setting in this standard framework of FDA, we need to know how to segment the curve, or the time series, into successive periods, which is not trivial in practice when there is unknown reparametrization and phase variations in the signal, see for instance Bonis et al. (2024). The advantage of our approach is precisely that it avoids this additional step of segmentation.

### 3.3.5. Discussion on possible extensions

The literature on functional central limit theorems for dependent data is rich in results for various functional classes and dependence assumptions. We believe it might be possible to use more recent and stronger results than Bühlmann (1995, Theorem 1). This would allow us to relax the decay of  $\beta_W$  from an exponential to a polynomial one. For instance, Radulović (1996, Theorem 1) is written for VC-classes functionals, but the proof seems to rely on the bracketing entropy bound that the functionals considered in the present work also satisfy.

Another natural extension to Theorem 3.10 is the framework of non stationary time series for Model 2. Although the times series  $(X_n)_{n \geq 1}$  is non stationary, we still define the topological signature  $F_M$  with as initial measure the invariant measure  $\pi_2$ . According to (Doukhan, 1994, Theorem 1, Section 2.4), the Markov Chain  $(\text{frac}(\gamma_n), V_n)_{n \geq 1}$  is  $\phi$ -mixing and also uniformly ergodic. We can then show convergence results quite directly only based on Markov chain properties. To keep things simple, let us consider Model 2 with no noise ( $W_n = 0$ ). Then,  $(\text{frac}(\gamma_n), V_n)$  admits a Central Limit Theorem (CLT), as well as  $(\phi(\text{frac}(\gamma_n)))_{n \geq 1}$ , see for instance Theorem 24 and Proposition 29 in Roberts and Rosenthal (2004). From this we can deduce that  $\hat{F}_{M,N}$  admits a pointwise CLT, meaning for fixed  $u$ .

If we now consider mixing properties of Model 2 (with additive noise  $W_n$ ), several avenues of research are still possible to demonstrate CLTs under non stationary regime. For instance, a CLT for  $\phi$ -mixing sequences was obtained in Utev (1990), by assuming the Lindeberg condition. In Rio (1997), a CLT for strong mixing is given that applies to both non-stationary sequences and triangular array settings (see also Rio, 2017). More recently, a functional CLT is proposed Merlevède and Peligrad (2020) for non-stationary strongly mixing sequences. This last contribution certainly paves the way for demonstrating a result analogous to (26) in a non-stationary setting.

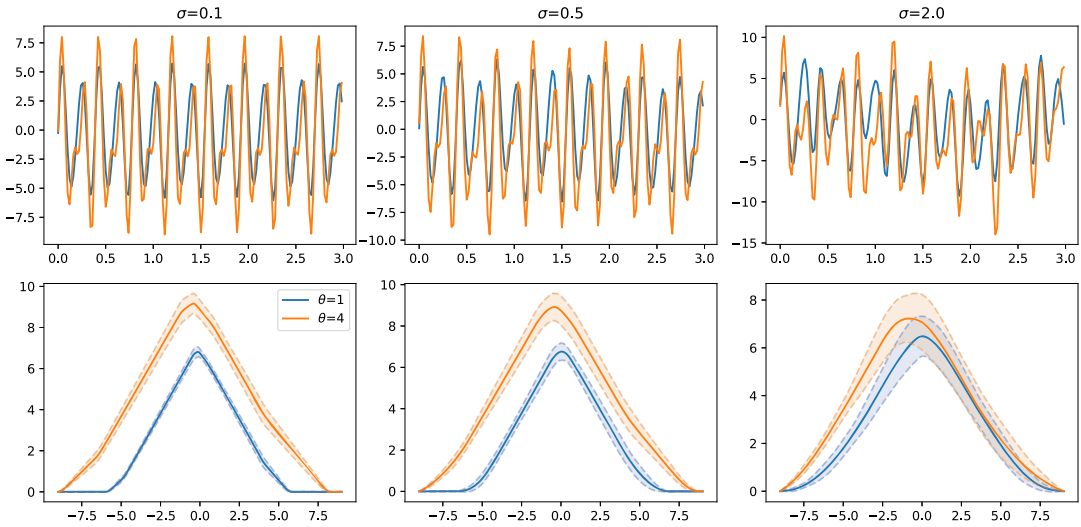


**Figure 6.** Signatures of  $\phi_1$  and  $\phi_4$ , estimated on reparametrized signals described above. The top row shows the first 3-second window from the 30-second signal, for both functions. The bottom row shows the estimated signatures and the confidence intervals.

## 4. Numerical illustration

To illustrate the signatures and their stability, we propose to estimate the signatures of processes with different periodic functions. Then, we compare the estimate to the signature of a process with a different reparametrizations.

We will consider periodic functions  $\phi_1$  and  $\phi_4$  defined by

$$\phi_\theta = \theta(\sin(6\pi t) + |t - \lfloor t \rfloor - \frac{1}{2}| - \frac{1}{2}) + 5 \sin(4\pi t), \quad \text{for } \theta \in \mathbb{R}.$$

The observed signal follows the discrete model (21), with  $T = 30$  seconds and a sampling rate of 50Hz. The reparametrizations are generated by integrating twice a Markov chain of accelerations, with a truncated Gaussian transition kernel. The noise is a Gaussian process with covariance

$$\Gamma(s, t) = \sigma^2 \exp\left(-\frac{(s - t)^2}{2\tau^2}\right).$$

We fix the temporal scale  $\tau$ , but we vary  $\sigma = 0.1, 0.5, 2$ , to illustrate the impact of noise on the signature.

For  $\bar{\rho}$ , we take the persistence silhouette introduced in Example 2.9, where the weights are given by the 0.2-truncated 1-persistence ( $\epsilon = 0.2$ ,  $p = 1$ ) and we use the projection  $\pi_{-9,9}$  as in (10). We infer the signatures on 3-second windows ( $M = 3 \cdot 50$ ). We construct the 1%-confidence intervals by resampling 200 times, with block lengths of 2 seconds ( $L = 2 \cdot 50$ ).

In Figure 6, for the same random realization  $\gamma_1$ , we calculate the empirical signature  $\hat{F}$  for  $\phi_1$  and  $\phi_4$ , and estimate the corresponding confidence intervals for  $F$ . For low noise levels, the variance due to the number of observations and the variability in the endpoints is small, compared to the difference between the functionals. As the noise level increases, the observed function loses its recurrent appearance and the signatures become dominated by the noise.

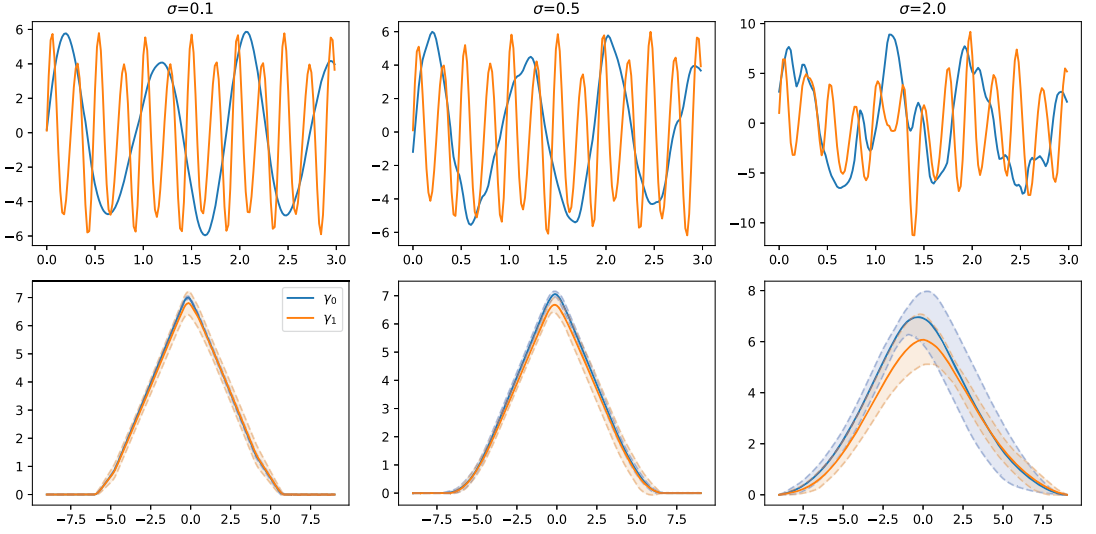


**Figure 7.** Signatures of  $\phi_1$ , estimated on two different reparametrized observations. The top row shows the first 3-second window from the two observed signals. The bottom row shows the estimated signatures and the confidence intervals.

Consider now two observations with the same periodic function  $\phi_1$ , but different reparametrizations  $\gamma_1, \gamma_2$ . In Figure 7, we can see that for small values of noise, the signatures are close, what confirms their invariance to reparametrization. It is worth noting that the signals contain different numbers of periods. For more noisy observations, the signatures lose the robustness.

## Appendix A: Moments of the Hölder constant of a stochastic process

Let  $(W_t)_{t \in [0, T]}$  be a stochastic process. A path  $t \mapsto W_t(\omega)$  is said to be  $\alpha$ -Hölder if  $|W_t(\omega) - W_s(\omega)| \leq \Lambda_{W(\omega)} |s - t|^\alpha$ , for any  $s, t \in [0, T]$ . Many processes, for example Gaussian processes, do not admit a uniform constant. Based on [Azaïs and Wschebor \(2009\)](#), [Hu and Le \(2013\)](#), [Shevchenko \(2017\)](#), we will now give a condition under which  $\Lambda_{W(\omega)}$  is a random variable and we will calculate its moments.

**Proposition A.1** ([Azaïs and Wschebor \(2009, Proposition 1.11\)](#)). *Suppose  $W$  satisfies (18) with  $K_{r_2, r_1}$  and let  $\alpha \in ]0, r_1/r_2[$ . Then, there exists a version  $(W'_t)_{t \in [0, 1]}$  of  $W$  and a random variable  $\Lambda_{W', \alpha} > 0$ , such that, for all  $s, t \in [0, 1]$ ,*

$$P(|W'_t - W'_s| \leq \Lambda_{W', \alpha} |t - s|^\alpha) = 1 \quad \text{and} \quad P(W_t = W'_t) = 1.$$

**Theorem A.2** ([Shevchenko \(2017\)](#)). *Let  $r_2 \in \mathbb{N}$  be such that  $K_{r_2, r_2} < \infty$  and  $1 - \alpha > 1/r_2$ ,  $r_2 \geq 2$ ,*

$$\mathbb{E}[\Lambda_W] \leq 16 \frac{\alpha+1}{\alpha} T K_{r_2, r_2}^{1/r_2} \alpha + 1.$$

In addition,

$$\mathbb{E}[\Lambda_W^k] \leq \begin{cases} \left(2^{3+2/r_2} \frac{\alpha+2/r_2}{\alpha}\right)^k K_{r_2, r_2\alpha+1}^k, & \text{for } 0 < k \leq r_2, \\ \left(2^{3+2/r_2} \frac{\alpha+2/r_2}{\alpha}\right)^k K_{k, k(\alpha+2/r_2)-1}, & \text{for } k > r_2. \end{cases}$$

**Lemma A.3 (Garsia–Rodemich–Rumsey Inequality (Hu and Le, 2013, Lemma 1.1)).** Let  $G : \mathbb{R}_+ \rightarrow \mathbb{R}_+$  be a non-decreasing function with  $\lim_{x \rightarrow \infty} G(x) = \infty$  and  $\delta : [0, T] \rightarrow [0, T]$  continuous and non-decreasing with  $\delta(0) = 0$ . Let  $G^{-1}$  and  $\delta^{-1}$  be lower-inverses. Let  $f : [0, T] \rightarrow \mathbb{R}$  be a continuous functions such that

$$\int_0^T \int_0^T G\left(\frac{|f(x) - f(y)|}{\delta(x - y)}\right) dx dy \leq B < \infty.$$

Then, for any  $s, t \in [0, T]$ ,

$$|f(s) - f(t)| \leq 8 \int_0^{|s-t|} G^{-1}(4B/u^2) d\delta(u).$$

**Proof of Theorem A.2.** Consider a path  $W(\omega)$  of the stochastic process and set

$$B(\omega) := \int_0^T \int_0^T G(|W_t(\omega)W_s(\omega)|/\delta(t-s)) dt ds,$$

where  $G(u) = u^{r_2}$  and  $\delta(u) = u^{\alpha+2/r_2}$ . Then,  $G^{-1}(u) = u^{1/r_2}$  and  $d\delta/du = (\alpha + 2/r_2)u^{\alpha+2/r_2-1}$ . Applying Lemma A.3,

$$\begin{aligned} |W_t(\omega) - W_s(\omega)| &\leq 8 \int_0^{|s-t|} G^{-1}(4B(\omega)/u^2) d\delta(u) \\ &\leq 8 \int_0^{|t-s|} \left(\frac{4B(\omega)}{u^2}\right)^{1/r_2} (\alpha + 2/p)u^{\alpha+2/r_2-1} du \\ &\leq 8(4B(\omega))^{1/r_2} (\alpha + 2/r_2) \int_0^{|t-s|} u^{\alpha-1} du \\ &= 8(4B(\omega))^{1/r_2} \frac{\alpha+2/r_2}{\alpha} |t-s|^\alpha. \end{aligned}$$

As this is valid for any  $s, t \in [0, T]$ ,  $\Lambda_W(\omega) \leq 8(4B(\omega))^{1/r_2} (\alpha + 2/r_2)/\alpha$ . By Jensens' inequality,

$$\mathbb{E}[\Lambda_W] \leq 2^{3+2/r_2} \frac{\alpha+2/r_2}{\alpha} \mathbb{E}[B(\omega)^{1/r_2}] \leq 2^{3+2/r_2} \frac{\alpha+2/r_2}{\alpha} \mathbb{E}[B(\omega)]^{1/r_2}. \quad (29)$$

By linearity of expectation,

$$\begin{aligned} \mathbb{E} \left[ \int_0^T \int_0^T G\left(\frac{|W_t(\omega)W_s(\omega)|}{\delta(t-s)}\right) dt ds \right] &= \int_0^T \int_0^T \frac{\mathbb{E}[|W_t(\omega)W_s(\omega)|^{r_2}]}{\delta(t-s)^{r_2}} dt ds \\ &= \int_0^T \int_0^T \frac{\mathbb{E}[|W_t(\omega)W_s(\omega)|^{r_2}]}{|t-s|^{p\alpha+2}} dt ds \\ &\leq \int_0^T \int_0^T K_{p, p\alpha+1} dt ds \end{aligned}$$

$$= T^2 K_{r_2, r_2\alpha+1}.$$

Finally,  $\mathbb{E}[\Lambda_W] \leq 2^{3+2/r_2} T^{2/r_2} K_{r_2, r_2\alpha+1}^{1/r_2} (\alpha + 2/r_2)/\alpha$ , as long as  $r_2\alpha + 1 \leq r_2$  and we can simplify the constants if  $r_2 > 2$ . Consider now the higher moments. If  $k \leq r_2$ , we can still apply Jensens' inequality in (29):

$$\begin{aligned} \mathbb{E}[\Lambda_W^k] &\leq \left( 2^{3+2/r_2} \frac{\alpha+2/r_2}{\alpha} \right)^k \mathbb{E}[B(\omega)^{k/r_2}] \\ &\leq \left( 2^{3+2/r_2} \frac{\alpha+2/r_2}{\alpha} \right)^k \mathbb{E}[B(\omega)]^{k/r_2} \\ &\leq \left( 2^{3+2/r_2} \frac{\alpha+2/r_2}{\alpha} \right)^k K_{r_2, r_2\alpha+1}^{k/r_2}. \end{aligned}$$

However, if  $k \geq r_2$ ,

$$\begin{aligned} \mathbb{E} \left[ \left( \int_0^T \int_0^T G \left( \frac{|W_t(\omega)W_s(\omega)|}{\delta(t-s)} \right) dt ds \right)^{k/r_2} \right] &= \int_0^T \int_0^T \frac{\mathbb{E}[|W_t(\omega)W_s(\omega)|^k]}{\delta(t-s)^k} dt ds \\ &= \int_0^T \int_0^T \frac{\mathbb{E}[|W_t(\omega)W_s(\omega)|^k]}{|t-s|^{k\alpha+2k/r_2}} dt ds \\ &\leq \int_0^T \int_0^T K_{k, k(\alpha+2/r_2)-1} dt ds \\ &= T^2 K_{k, k(\alpha+2/r_2)-1}. \end{aligned} \quad \square$$

## Appendix B: Stationary regimes for the time series models

### B.1. Model 1 is stationary

In this section, we check that  $(\text{frac}(\gamma_n))_{n \in \mathbb{N}}$  is stationary. It is sufficient to show that for any  $K \geq 1$ ,  $(\text{frac}(\gamma_0), \dots, \text{frac}(\gamma_K)) \sim (\text{frac}(\gamma_n), \dots, \text{frac}(\gamma_{n+K}))$ , for any  $n \geq 0$ . We write

$$(\text{frac}(\gamma_n), \dots, \text{frac}(\gamma_{n+K})) = \text{frac}(\text{frac}(\gamma_0 + \sum_{r=0}^{n-1} V_r) + \text{frac}(0, V_n, \dots, \sum_{r=n}^{n+K-1} V_r)),$$

and we analyze the two terms separately. Here,  $\text{frac}$  is applied component-wise. First, because  $(V_n)_{n \in \mathbb{N}}$  are i.i.d.,  $(\sum_{r=0}^k V_r) \sim (\sum_{r=n}^{n+k} V_r)$ , for any  $n, k \in \mathbb{N}$ . Thus  $(0, V_0, \dots, \sum_{r=0}^{n-1} V_r) \sim (0, V_n, \dots, \sum_{r=n}^{n+K-1} V_r)$ . It also remains true when we apply  $\text{frac}$  component-wise, because it is a measurable mapping  $\mathbb{R}^{K+1} \rightarrow \mathbb{R}^{K+1}$ . Second, we claim the following lemma on the sum of two random variables, one of which is uniform.

**Lemma B.1.** *If  $U \sim \mathcal{U}([0, 1])$  and  $Z$  is a real-valued random variable independent of  $U$ , then  $\text{frac}(U + Z) \sim \text{frac}(U) \sim U$ .*

Before showing Lemma B.1, we conclude the proof by applying it to  $U = \gamma_0$  and  $Z = \sum_{r=0}^{n-1} V_r$ . Indeed,  $\gamma_0$  is independent from  $(V_r)_{r=0}^{n-1}$ , so we obtain that  $\text{frac}(\gamma_0) \sim \text{frac}(\gamma_0 + \sum_{r=0}^{n-1} V_r)$ . Finally, com-



binning the above with  $\text{frac}((0, V_0, \dots, \sum_{r=0}^{n-1} V_r)) \sim \text{frac}((0, V_n, \dots, \sum_{r=n}^{n+K-1} V_r))$ , we have that  $\text{frac}(\gamma_0, \dots, \gamma_K) \sim \text{frac}(\gamma_n, \dots, \gamma_{n+K})$ .

**Proof of Lemma B.1.** First, it is clear that for  $s \leq 0$ ,  $P(\text{frac}(U + Z) < s) = 0$  and that for  $s > 1$ ,  $1 \geq P(\text{frac}(U + Z) < s) \geq P(\text{frac}(U + Z) \leq 1) = 1$ . For  $0 < s < 1$ ,

$$P(\text{frac}(U + Z) \leq s) = P\left(U + Z \in \bigcup_{k \in \mathbb{Z}} [k, k + s]\right) = \sum_{k \in \mathbb{Z}} P(U + Z \in [k, k + s]). \quad (30)$$

Because  $U$  and  $Z$  are independent,  $P(U + Z \in [k, k + s]) = (\mu_U \star \mu_Z)([k, k + s])$ , where  $\mu_U$  and  $\mu_Z$  are the probability measures of  $U$  and  $Z$  respectively and  $\star$  denotes their convolution. Note that since  $\mu$  is translation-invariant,

$$\begin{aligned} (\mu_U \star \mu_Z)([k, k + s]) &= \int_{\mathbb{R}} \int_0^1 1_{[k, k+s]}(z + u) du d\mu_Z(z) \\ &= \int_{\mathbb{R}} \mu([0, 1] \cap [k - z, k + s - z]) d\mu_Z(z) \\ &= \int_{\mathbb{R}} \mu([-k, -k + 1] \cap [-z, -z + s]) d\mu_Z(z) \\ &= \int_{\mathbb{R}} \mu([-k, -k + 1] \cap [-z, -z + s]) d\mu_Z(z). \end{aligned}$$

Going back to (30),

$$\begin{aligned} P(\text{frac}(U + Z) \leq s) &= \sum_{k \in \mathbb{Z}} \int_{\mathbb{R}} \mu([-k, -k + 1] \cap [-z, -z + s]) d\mu_Z(z) \\ &= \int_{\mathbb{R}} \sum_{k \in \mathbb{Z}} \mu([-k, -k + 1] \cap [-z, -z + s]) d\mu_Z(z) \\ &= \int_{\mathbb{R}} \mu([-z, -z + s]) d\mu_Z(z) \\ &= \mu([0, s]) \int_{\mathbb{R}} d\mu_Z(z). \\ &= s. \end{aligned}$$

Therefore, the distribution function of  $\text{frac}(U + Z)$  is uniform on  $[0, 1]$  and therefore also equal to that of  $\text{frac}(U)$ .  $\square$

## B.2. Stationary distribution for Model 2

The process  $(\text{frac}(\gamma_n))_{n \in \mathbb{N}}$  is defined in (22), via the Markov chain  $(V_n)_{n \in \mathbb{N}}$ . Recall that this Markov chain has a transition probability kernel  $P$ , with support included in  $I = [v_{\min}, v_{\max}]$ . The time series  $(\text{frac}(\gamma_n))_{n \in \mathbb{N}}$  is not itself a Markov Chain but it can be easily checked that  $(\text{frac}(\gamma_n), V_n)_{n \geq 1}$  is. Let  $\tilde{P}$  be the transition kernel of this Markov Chain and let  $\mathcal{U}$  be the uniform measure on  $[0, 1] \times I$ . By applying a similar proof as the proof of Doeblin's Condition for Model 2, see Section B.2 step 8 in

the supplement [Chazal, Michel and Reise \(2025\)](#), it can be shown that for any  $x \in [0, 1] \times I$ , whenever  $A \in \mathcal{B}([0, 1] \times I)$  is such that  $\mathcal{U}(A) > 0$ , then  $P^n(x, A) > 0$  for some  $n$  sufficiently big. In other terms, the Markov Chain  $(\text{frac}(\gamma_n), V_n)_{n \geq 0}$  is  $\mathcal{U}$ -irreducible.

By Proposition 4.2.2 [Meyn and Tweedie \(2012\)](#), there is a maximal measure,  $Q$ , for which  $(\text{frac}(\gamma_n), V_n)_{n \geq 0}$  is  $Q$ -irreducible. By Theorem 8.3.4 in [Meyn and Tweedie \(2012\)](#), such a maximally-irreducible chain is either transient or recurrent. The fact that we can reach any element from the cover from any other one, as well as the compactity of the domain  $[0, 1]$  prevents transience, so we can conclude it is recurrent. A recurrent chain admits an invariant measure, by Theorem 10.0.1 [Meyn and Tweedie \(2012\)](#).

## Appendix C: Gaussian approximation for dependent data

**Theorem C.1** ([Kosorok \(2008, Theorem 11.24\)](#)). *Let  $(X_n)_{n \in \mathbb{N}} \subset \mathbb{R}^d$  be a stationary sequence and consider a functional family  $\mathcal{F} = (F_t)_{t \in \mathbb{U}}$  with finite bracketing entropy. Suppose there exists  $r \in ]2, \infty[$ , such that*

$$\sum_{k=1}^{\infty} k^{\frac{2}{r-2}} \beta_X(k) < \infty. \quad (31)$$

*Then,  $\sqrt{N}(\hat{F}_t - F_t)$  converges to a tight, zero-mean Gaussian  $G$  process with covariance (27).*

**Theorem C.2** ([Bühlmann \(1995, Theorem1\)](#)). *Let  $(X_n)_{n \in \mathbb{N}} \subset \mathbb{R}^d$  be a stationary sequence and consider a functional family  $\mathcal{F} = (F_t)_{t \in \mathbb{U}}$  with finite bracketing entropy. Suppose that  $\beta_X(k) \xrightarrow[k \rightarrow \infty]{} 0$  decrease exponentially and that  $\mathcal{F}$  satisfies (6,8). Let the bootstrap sample be generated with the Moving Block Bootstrap, where the block size  $L(n)$  satisfying  $L(n) \rightarrow \infty$  and  $L(n) = O(n^{1/2-\epsilon})$  for some  $0 < \epsilon < 1/2$ . Then,*

$$\sqrt{N}(\hat{F}_N^* - \mathbb{E}^*[\hat{F}_N^*]) \rightarrow^* G \quad \text{in probability,}$$

*where  $G$  is the zero-mean Gaussian Process with the covariance (27).*

## Acknowledgments

The authors are grateful to numerous colleagues for the fruitful discussions and they wish to particularly thank Paul Doukhan, Giovanni Peccati, Alex Delalande, Quentin Mériçot and Daniel Perez.

## Funding

WR was supported by TopAI ANR-19-CHIA-0001 and BM by GeoDSIC ANR-22-CE40-0007.

## Supplementary Material

**Supplement to “Topological signatures of periodic-like signals”** (DOI: [10.3150/24-BEJ1793SUPP](https://doi.org/10.3150/24-BEJ1793SUPP); .pdf). The supplement [Chazal, Michel and Reise \(2025\)](#) contains the calculations of Lipschitz constants of  $\bar{\rho}$  from Examples 2.9 and 2.10, the proof of Proposition 3.11 as well as technical details for the proof of Theorem 3.10.

## References

- Adams, H., Emerson, T., Kirby, M., Neville, R., Peterson, C., Shipman, P., Chepushtanova, S., Hanson, E., Motta, F. and Ziegelmeier, L. (2017). Persistence images: A stable vector representation of persistent homology. *J. Mach. Learn. Res.* **18** Paper No. 8. [MR3625712](#)
- Azaïs, J.-M. and Wschebor, M. (2009). *Level Sets and Extrema of Random Processes and Fields*. Hoboken, NJ: Wiley. [MR2478201](#) <https://doi.org/10.1002/9780470434642>
- Berry, E., Chen, Y.-C., Cisewski-Kehe, J. and Fasy, B.T. (2020). Functional summaries of persistence diagrams. *J. Appl. Comput. Topol.* **4** 211–262. [MR4096338](#) <https://doi.org/10.1007/s41468-020-00048-w>
- Bogachev, V.I. (2007). *Measure Theory. Vol. I, II*. Berlin: Springer. [MR2267655](#) <https://doi.org/10.1007/978-3-540-34514-5>
- Bois, A., Tervil, B., Moreau, A., Vienne-Jumeau, A., Ricard, D. and Oudre, L. (2022). A topological data analysis-based method for gait signals with an application to the study of multiple sclerosis. *PLoS ONE* **17** 1–23. <https://doi.org/10.1371/journal.pone.0268475>
- Bonis, T., Chazal, F., Michel, B. and Reise, W. (2024). Topological phase estimation method for reparameterized periodic functions. *Adv. Comput. Math.* **50** Paper No. 66. [MR4770431](#) <https://doi.org/10.1007/s10444-024-10157-0>
- Bubenik, P. (2015). Statistical topological data analysis using persistence landscapes. *J. Mach. Learn. Res.* **16** 77–102. [MR3317230](#)
- Bühlmann, P. (1995). The blockwise bootstrap for general empirical processes of stationary sequences. *Stochastic Process. Appl.* **58** 247–265. [MR1348377](#) [https://doi.org/10.1016/0304-4149\(95\)00019-4](https://doi.org/10.1016/0304-4149(95)00019-4)
- Bühlmann, P. (2002). Bootstraps for time series. *Statist. Sci.* **17** 52–72. [MR1910074](#) <https://doi.org/10.1214/ss/1023798998>
- Carrière, M., Chazal, F., Ike, Y., Lacombe, T., Royer, M. and Umeda, Y. (2020). PersLay: A neural network nayer for persistence diagrams and new graph topological signatures. In *AISTATS'2017* **108** 2786–2796. PMLR.
- Chazal, F. and Michel, B. (2021). An introduction to topological data analysis: Fundamental and practical aspects for data scientists. *Front. Artif. Intell.* **4**. <https://doi.org/10.3389/frai.2021.667963>
- Chazal, F., Michel, B. and Reise, W. (2025). Supplement to “Topological signatures of periodic-like signals.” <https://doi.org/10.3150/24-BEJ1793SUPP>
- Chazal, F., Fasy, B.T., Lecci, F., Rinaldo, A. and Wasserman, L. (2014). Stochastic convergence of persistence landscapes and silhouettes. In *Computational Geometry (SoCG'14)* 474–483. New York: ACM. [MR3382329](#)
- Chazal, F., de Silva, V., Glisse, M. and Oudot, S. (2016). *The Structure and Stability of Persistence Modules. SpringerBriefs in Mathematics*. Cham: Springer. [MR3524869](#) <https://doi.org/10.1007/978-3-319-42545-0>
- Chung, Y.-M. and Lawson, A. (2022). Persistence curves: A canonical framework for summarizing persistence diagrams. *Adv. Comput. Math.* **48** Paper No. 6. [MR4368950](#) <https://doi.org/10.1007/s10444-021-09893-4>
- Cohen-Steiner, D., Edelsbrunner, H. and Harer, J. (2007). Stability of persistence diagrams. *Discrete Comput. Geom.* **37** 103–120. [MR2279866](#) <https://doi.org/10.1007/s00454-006-1276-5>
- Cohen-Steiner, D., Edelsbrunner, H., Harer, J. and Mileyko, Y. (2010). Lipschitz functions have  $L_p$ -stable persistence. *Found. Comput. Math.* **10** 127–139. [MR2594441](#) <https://doi.org/10.1007/s10208-010-9060-6>
- Corcoran, P. and Jones, C. (2017). Modelling topological features of swarm behaviour in space and time with persistence landscapes. *IEEE Access* **5** 18534–18544. <https://doi.org/10.1109/ACCESS.2017.2749319>
- Dedecker, J., Doukhan, P., Lang, G., José Rafael, L.R., Louhichi, S. and Prieur, C. (2007). *Weak Dependence: With Examples and Applications. Lecture Notes in Statistics* **190**. New York: Springer. [MR2338725](#)
- Divol, V. and Polonik, W. (2019). On the choice of weight functions for linear representations of persistence diagrams. *J. Appl. Comput. Topol.* **3** 249–283. [MR3996956](#) <https://doi.org/10.1007/s41468-019-00032-z>
- Doukhan, P. (1994). *Mixing: Properties and Examples. Lecture Notes in Statistics* **85**. New York: Springer. [MR1312160](#) <https://doi.org/10.1007/978-1-4612-2642-0>
- Fernández, X. and Mateos, D. (2022). Topological biomarkers for real-time detection of epileptic seizures. ArXiv preprint. Available at [arXiv:2211.02523](https://arxiv.org/abs/2211.02523). <https://doi.org/10.1214/aos/1069362747>
- Ghil, M. and Sciamarella, D. (2023). Review article: Dynamical systems, algebraic topology, and the climate sciences. *EGUsphere*. Preprint. <https://doi.org/10.5194/egusphere-2023-216>
- Gidea, M. and Katz, Y. (2018). Topological data analysis of financial time series: Landscapes of crashes. *Phys. A* **491** 820–834. [MR3721543](#) <https://doi.org/10.1016/j.physa.2017.09.028>

- Goldberger, A.L., Amaral, L.A., Glass, L., Hausdorff, J.M., Ivanov, P.C., Mark, R.G., Mietus, J.E., Moody, G.B., Peng, C.K. and Stanley, H.E. (2000). PhysioBank, PhysioToolkit, and PhysioNet: Components of a new research resource for complex physiologic signals. *Circulation* **101** E215–220. <https://doi.org/10.1161/01.cir.101.23.e215>
- Hu, Y. and Le, K. (2013). A multiparameter Garsia-Rodemich-Rumsey inequality and some applications. *Stochastic Process. Appl.* **123** 3359–3377. [MR3071383 https://doi.org/10.1016/j.spa.2013.04.019](https://doi.org/10.1016/j.spa.2013.04.019)
- Khasawneh, F.A. and Munch, E. (2016). Chatter detection in turning using persistent homology. *Mech. Syst. Signal Process.* **70–71** 527–541. <https://doi.org/10.1016/j.ymssp.2015.09.046>
- Khorram, S., McInnis, M.G. and Provost, E.M. (2019). Trainable time warping: Aligning time-series in the continuous-time domain. In *ICASSP'2019* 3502–3506. <https://doi.org/10.1109/ICASSP.2019.8682322>
- Kosorok, M.R. (2008). *Introduction to Empirical Processes and Semiparametric Inference*. Springer Series in Statistics. New York: Springer. [MR2724368 https://doi.org/10.1007/978-0-387-74978-5](https://doi.org/10.1007/978-0-387-74978-5)
- Krebs, J. (2021). On limit theorems for persistent Betti numbers from dependent data. *Stochastic Process. Appl.* **139** 139–174. [MR4260054 https://doi.org/10.1016/j.spa.2021.04.013](https://doi.org/10.1016/j.spa.2021.04.013)
- Marron, J.S., Ramsay, J.O., Sangalli, L.M. and Srivastava, A. (2015). Functional data analysis of amplitude and phase variation. *Statist. Sci.* **30** 468–484. [MR3432837 https://doi.org/10.1214/15-STS524](https://doi.org/10.1214/15-STS524)
- Merlevède, F. and Peligrad, M. (2020). Functional CLT for nonstationary strongly mixing processes. *Statist. Probab. Lett.* **156** 108581. [MR4003491 https://doi.org/10.1016/j.spl.2019.108581](https://doi.org/10.1016/j.spl.2019.108581)
- Meyn, S.P. and Tweedie, R.L. (2012). *Markov Chains and Stochastic Stability*. Springer Science & Business Media.
- Panaretos, V.M. and Zemel, Y. (2020). *An Invitation to Statistics in Wasserstein Space*. SpringerBriefs in Probability and Mathematical Statistics. Cham: Springer. [MR4350694 https://doi.org/10.1007/978-3-030-38438-8](https://doi.org/10.1007/978-3-030-38438-8)
- Perea, J.A. (2019). Topological times series analysis. *Notices Amer. Math. Soc.* **66** 686–694. [MR3929469](https://doi.org/10.1090/ICDE.2000.839385)
- Perez, D. (2022). On  $C^0$ -persistent homology and trees. ArXiv preprint. Available at [arXiv:2012.02634v3](https://arxiv.org/abs/2012.02634v3).
- Perng, C.S., Wang, H., Zhang, S.R. and Parker, D.S. (2000). Landmarks: A new model for similarity-based pattern querying in time series databases. In *ICDE'00* 33–42. San Diego, CA, USA: IEEE Comput. Soc. <https://doi.org/10.1109/ICDE.2000.839385>
- Pettis, B.J. (1938). On integration in vector spaces. *Trans. Amer. Math. Soc.* **44** 277–304. [MR1501970 https://doi.org/10.2307/1989973](https://doi.org/10.2307/1989973)
- Plonka, G. and Zheng, Y. (2016). Relation between total variation and persistence distance and its application in signal processing. *Adv. Comput. Math.* **42** 651–674. [MR3502107 https://doi.org/10.1007/s10444-015-9438-8](https://doi.org/10.1007/s10444-015-9438-8)
- Radulović, D. (1996). The bootstrap for empirical processes based on stationary observations. *Stochastic Process. Appl.* **65** 259–279. [MR1425360 https://doi.org/10.1016/S0304-4149\(96\)00102-0](https://doi.org/10.1016/S0304-4149(96)00102-0)
- Ramsay, J.O. and Silverman, B.W. (2002). *Applied Functional Data Analysis: Methods and Case Studies*. Springer Series in Statistics. New York: Springer. [MR1910407 https://doi.org/10.1007/b98886](https://doi.org/10.1007/b98886)
- Reise, W. (2023). Topological techniques for inference on periodic functions with phase variation Ph.D. thesis Université Paris-Saclay.
- Rio, E. (1997). About the Lindeberg method for strongly mixing sequences. *ESAIM Probab. Stat.* **1** 35–61. [MR1382517 https://doi.org/10.1051/ps:1997102](https://doi.org/10.1051/ps:1997102)
- Rio, E. (2017). *Asymptotic Theory of Weakly Dependent Random Processes*. Probability Theory and Stochastic Modelling **80**. Berlin: Springer. [MR3642873 https://doi.org/10.1007/978-3-662-54323-8](https://doi.org/10.1007/978-3-662-54323-8)
- Roberts, G.O. and Rosenthal, J.S. (2004). General state space Markov chains and MCMC algorithms. *Probab. Surv.* **1** 20–71. [MR2095565 https://doi.org/10.1214/154957804100000024](https://doi.org/10.1214/154957804100000024)
- Shevchenko, G. (2017). Kolmogorov continuity theorem and Holder norm. MathOverflow. Available at <https://mathoverflow.net/q/279085> (version: 2017-08-19).
- Su, J., Kurtek, S., Klassen, E. and Srivastava, A. (2014). Statistical analysis of trajectories on Riemannian manifolds: Bird migration, hurricane tracking and video surveillance. *Ann. Appl. Stat.* **8** 530–552. [MR3192001 https://doi.org/10.1214/13-AOAS701](https://doi.org/10.1214/13-AOAS701)
- Tang, R. and Müller, H.-G. (2008). Pairwise curve synchronization for functional data. *Biometrika* **95** 875–889. [MR2461217 https://doi.org/10.1093/biomet/asn047](https://doi.org/10.1093/biomet/asn047)
- Utev, S.A. (1990). Central limit theorem for dependent random variables. In *Probability Theory and Mathematical Statistics, Vol. II (Vilnius, 1989)* 519–528. Vilnius: “Mokslas”. [MR1153906](https://doi.org/10.1214/aos/1069362747)
- Wang, K. and Gasser, T. (1997). Alignment of curves by dynamic time warping. *Ann. Statist.* **25** 1251–1276. [MR1447750 https://doi.org/10.1214/aos/1069362747](https://doi.org/10.1214/aos/1069362747)